

KfK 5109  
Dezember 1992

**Tritium Release of  $\text{Li}_4\text{SiO}_4$ ,  $\text{Li}_2\text{O}$   
and Beryllium and Chemical  
Compatibility of Beryllium with  
 $\text{Li}_4\text{SiO}_4$ ,  $\text{Li}_2\text{O}$  and Steel  
(SIBELIUS Irradiation)**

W. Dienst, D. Schild, H. Werle  
Institut für Neutronenphysik und Reaktortechnik  
Institut für Materialforschung  
Hauptabteilung Versuchstechnik  
Projekt Kernfusion  
Association KfK-EURATOM

**Kernforschungszentrum Karlsruhe**



Kernforschungszentrum Karlsruhe  
Institut für Neutronenphysik und Reaktortechnik  
Institut für Materialforschung  
Hauptabteilung Versuchstechnik  
Projekt Kernfusion  
Association KfK - EURATOM

KfK 5109

Tritium Release of  $\text{Li}_4\text{SiO}_4$ ,  $\text{Li}_2\text{O}$  and Beryllium and  
Chemical Compatibility of Beryllium with  $\text{Li}_4\text{SiO}_4$ ,  $\text{Li}_2\text{O}$  and  
Steel (SIBELIUS Irradiation)

W. Dienst, D. Schild and H. Werle

Kernforschungszentrum Karlsruhe GmbH, Karlsruhe

Als Manuskript gedruckt  
Für diesen Bericht behalten wir uns alle Rechte vor

Kernforschungszentrum Karlsruhe GmbH  
Postfach 3640, 7500 Karlsruhe 1

ISSN 0303-4003

## **Tritium Release of $\text{Li}_4\text{SiO}_4$ , $\text{Li}_2\text{O}$ and Beryllium and Chemical Compatibility of Beryllium with $\text{Li}_4\text{SiO}_4$ , $\text{Li}_2\text{O}$ and Steel (SIBELIUS Irradiation)**

### **Abstract**

The objective of the SIBELIUS irradiation, a joint EC-US project performed at CEN Grenoble, was to investigate the oxidation kinetics of beryllium in contact with ceramic and the nature and extent of beryllium interaction with steel in a neutron environment.

In this work post irradiation examinations of SIBELIUS specimens performed at KfK are described. Tritium release of  $\text{Li}_4\text{SiO}_4$ ,  $\text{Li}_2\text{O}$  and beryllium was studied by out-of-pile annealing and chemical compatibility of beryllium with  $\text{Li}_4\text{SiO}_4$ ,  $\text{Li}_2\text{O}$  and steel by microscopic examinations.

Tritium release of the ceramics was found to be consistent with SIBELIUS in-pile observations and previous tests. Release of tritium generated in beryllium was found to be very slow, in accordance with previous work. For beryllium which was in contact with ceramic during irradiation, a second type of tritium, caused by injection of 2.7 MeV tritons generated in the ceramic, is observed. Release of injected tritium is faster than that of generated. Evidence for injected tritium in beryllium was also found in the microscopic studies.

The observed minor chemical reactions of beryllium with steel and probably also those with breeder materials under neutron irradiation are consistent with the results of laboratory annealing tests.

## **Tritiumfreisetzung von $\text{Li}_4\text{SiO}_4$ , $\text{Li}_2\text{O}$ und Beryllium sowie chemische Verträglichkeit von Beryllium mit $\text{Li}_4\text{SiO}_4$ , $\text{Li}_2\text{O}$ und Stahl (SIBELIUS-Bestrahlungsexperiment)**

### **Zusammenfassung**

Das Ziel des SIBELIUS-Bestrahlungsexperiments, eines gemeinsamen EG-US Projekts, das im CEN Grenoble durchgeführt wurde, war die Untersuchung der Oxidationskinetik von Beryllium in Kontakt mit Keramik und von Art sowie Ausmaß der Wechselwirkung von Beryllium mit Stahl unter Neutronenbestrahlung.

In dieser Arbeit werden die bei KfK durchgeführten Nachuntersuchungen an SIBELIUS-Proben beschrieben. Die Tritiumfreisetzung von  $\text{Li}_4\text{SiO}_4$ ,  $\text{Li}_2\text{O}$  und Beryllium wurde durch out-of-pile Ausheizung und die chemische Verträglichkeit von Beryllium mit  $\text{Li}_4\text{SiO}_4$ ,  $\text{Li}_2\text{O}$  und Stahl wurde anhand mikroskopischer Aufnahmen untersucht.

Die Tritiumfreisetzungsmessungen an den Keramik-Proben sind konsistent mit SIBELIUS-in-pile-Ergebnissen und früheren Untersuchungen. Die Freisetzung des in Beryllium erzeugten Tritiums verläuft, in Übereinstimmung mit früheren Untersuchungen, sehr langsam. Beryllium-Proben, die während der Bestrahlung mit Keramik in Kontakt waren, enthalten eine zweite Art von Tritium, das durch Injektion von 2.7 MeV Tritonen, die in der Keramik erzeugt werden, hervorgerufen wird. Das injizierte Tritium wird schneller freigesetzt als das in Beryllium erzeugte. Auch die mikroskopischen Untersuchungen liefern Hinweise auf injiziertes Tritium in Beryllium.

Die beobachteten geringfügigen chemischen Wechselwirkungen von Beryllium unter Neutronenbestrahlung mit Stahl und wahrscheinlich auch die mit dem keramischen Brutmaterialien sind konsistent mit den Ergebnissen von Laborglühversuchen.

## Contents

1.	Introduction	1
2.	Irradiation	1
3.	Inpile tritium release	2
4.	Tritium annealing	3
4.1	Experimental	3
4.2	Ceramics	4
4.3	Beryllium	5
5.	Chemical compatibility of beryllium with breeder and cladding materials	8
5.1	Samples	8
5.2	Relevant results from previous annealing tests	8
5.3	Post-irradiation examination results	9
5.3.1	Beryllium with steel	9
5.3.2	Beryllium with breeder materials	9
6.	Conclusions	11
	Acknowledgements	11
	References	12
	Tables	14
	Figures	18

## 1. Introduction

Solid breeder blankets require the use of beryllium in order to achieve adequate tritium breeding. Among the concerns related to the use of beryllium are compatibility with other blanket materials (ceramic and steel), tritium retention and swelling.

The main objective of the SIBELIUS experiment [1,2], a common EC-US program, was to investigate the oxidation kinetics of beryllium in contact with ceramics and the nature and extent of beryllium interaction with steel in a neutron environment. In addition, tritium release characteristics of the ceramic/beryllium/steel compacts were checked in-pile and tritium and helium retention in beryllium was determined by out-of-pile annealing.

An extensive post-irradiation examination (PIE) program is performed by US laboratories, CEA and KfK. CEA PIE and in-pile results have been presented earlier [2,3]. SIBELIUS PIE work at KfK is described in this report and was concerned with tritium retention in beryllium and ceramics and with chemical compatibility of beryllium with ceramics and steel.

## 2. Irradiation

The design of irradiation device and the experimental conditions are reported in [1,2]. Eight capsules (inner diam. 8 mm) have been irradiated in SIBELIUS (fig. 1). Four of the eight capsules (no. 2, 3, 5, and 6) accommodated pellet stacks of ceramics, beryllium and steels. Each capsule accommodates a different ceramic, i.e.  $\text{Li}_4\text{SiO}_4$ ,  $\text{LiAlO}_2$ ,  $\text{Li}_2\text{O}$  and  $\text{Li}_4\text{SiO}_4$ . Capsule 1 contained, in addition to beryllium and steel pellets, a 4 mm thick bed of 0.45 - 0.56 mm  $\varnothing$   $\text{Li}_4\text{SiO}_4$  pebbles. Capsule 4 contained only three 12 mm high beryllium pellets for swelling tests, capsules 7 and 8 accommodated only  $\text{LiAlO}_2$  and  $\text{Li}_2\text{O}$  pellets for check purposes. The pellets of each stack are maintained in intimate contact by a graphite spring. Capsule 1 was not correctly mounted, resulting in a gap of 2 - 3 mm above the pebble bed. In fig. 1, the specimens studied at KfK, are indicated.

All capsules, except no. 4, were purged with  $\text{He} + 0.1\% \text{H}_2$ . The irradiation temperature was 550° C, except for the capsule with the  $\text{Li}_4\text{SiO}_4$  pebble bed. For this capsule the maximum ceramic temperature was about 470° C and that of the ceramic/beryllium interface about 270° C.

The beryllium pellets for compatibility tests (2 mm thick) studied here were made by Brush-Wellman (specification B-26, arc cast,  $\text{BeO} < 300 \text{ ppm}$ ). The structure is characterized by grains as large as 2 mm and some intergranular cracks. A cold

worked layer resulting from machining is observed on the surface [2]. The density determined from the masses and dimensions varied between 1.79 and 1.82 g/cm<sup>3</sup> and was in the average 1.805 g/cm<sup>3</sup> (98 % TD) [8].

Two types of steel pellets (2 mm thick) were used: 316 L austenitic (Cr 17.44, Ni 12.33, Mo 2.3, Mn 1.82 wt%) and 1.4914 martensitic (Cr 10.6, C 0.13, Ni 0.87, Mo 0.8 wt %).

Material properties of the ceramics investigated in this study are summarized in table 1, micrographs of the Li<sub>4</sub>SiO<sub>4</sub> and Li<sub>2</sub>O pellets after irradiation are shown in fig. 2.

The ceramic specimens were degassed at 600° C for four hours in vacuum to eliminate moisture, then all specimens were assembled in a dry glove box. Similar precautions were taken against moisture after irradiation: a moisture-tight argon enclosure was specially designed and installed in the hot cells for dismantling operations. Transport and handling of samples after irradiation was done under inert atmosphere.

The irradiation was performed in the core of the SILOE reactor at CEN Grenoble from April to October 1990 for 1690 h (4 reactor cycles). Neutron fluxes in the device midplane were: thermal 1.1.10<sup>14</sup>, fast (> 1 MeV) 1.0.10<sup>14</sup> 1/cm<sup>2</sup>s. Calculated beryllium dpa is 0.7 [2, 3]. Irradiation conditions for the capsules investigated at KfK are summarized in table 2.

### 3. Inpile tritium release [3]

Measured steady-state tritium release rates, which are equal to the production rates and sample temperatures are given in table 2. For capsules 1 and 5 the calculated production is in reasonable agreement with measurement, whereas for capsule 2 the calculated value is too high by 65 %.

Temperature transients to estimate tritium residence times have been performed for capsule 2 (Li<sub>4</sub>SiO<sub>4</sub> pellets/Be/steel), 3 (LiAlO<sub>2</sub> pellets/Be/steel), 6 (Li<sub>2</sub>ZrO<sub>3</sub> pellets/Be/steel) and 7 (LiAlO<sub>2</sub> pellets). Residence times are defined here as the time required for the normalized release rate  $(r - r_{ss}) / (r_{max} - r_{ss})$  to drop to 1/e (index ss refers to steady-state).

For LiAlO<sub>2</sub> residence times are in agreement for the two capsules (no. 3 and 7) and with previous tests. For Li<sub>2</sub>ZrO<sub>3</sub> too, residence times are comparable with previous data, whereas for the Li<sub>4</sub>SiO<sub>4</sub> pellets they are at 550 °C comparable, but

at 460 °C at least an order of magnitude larger than in previous tests ( $\approx 200$  compared to 5 - 10 h).

Because for  $\text{LiAlO}_2$  and  $\text{Li}_2\text{ZrO}_3$  contact with beryllium had no significant effect on tritium release, the large discrepancy of residence times for the SIBELIUS  $\text{Li}_4\text{SiO}_4$  pellets at 460 °C with previous results for other  $\text{Li}_4\text{SiO}_4$  samples is tentatively attributed to a bad quality of these pellets.

Also in beryllium some tritium is produced during irradiation. But because the generation rate is much smaller (about three order of magnitude) than that in the ceramics, tritium release from the stack correspond essentially to that from the ceramic.

## 4. Tritium annealing

### 4.1 Experimental

Annealing was performed in a device described earlier [9]. The main characteristics are: the sample chamber is connected by a short, heated line ( $\approx 300$  °C) to a Zn reductor (390 °C). The reductor transforms any tritium water to tritium gas. This avoids problems with tritium water adsorption and allows quantitative tritium measurements. The tritium activity is measured in parallel with an ionization chamber and a proportional counter. In all cases, the agreement between the two detectors is excellent. Therefore only the ionization chamber data are given.

The samples were purged with 50 standard-cm<sup>3</sup>/min He + 0.1 % H<sub>2</sub> (purity 99.9999 %). Two heating procedures were used: linear ramps with 5 °C/min up to about 850 °C, which is hold for  $\geq 3$  h or fast, stepwise temperature increase, holding each temperature level for about 2 h.

Annealing results are summarized in table 3. For the ceramics the residual inventory after annealing is negligible. The release from beryllium is slow even at 860 °C. Pellet 1 of capsule 1 was annealed at 860 °C for about 35 h (see table 3). During this period, the residence time increased from about 18 to 29 h with an average of 24 h. The residence time is defined here by  $\tau = (t_2 - t_1)/\ln(r_1/r_2)$  ( $t$  time,  $r$  release rate). Residual beryllium inventories at the end of annealing have been estimated by

$$I_{\text{res}} = r_0 \int_0^{\infty} e^{-t/\tau} dt = r_0 \tau$$

(end of annealing:  $t = 0$ ,  $r = r_0$ ;  $\tau = 24$  h). Total inventories are determined by summing up the measured release and the estimated residual inventory (table 3).

#### 4.2 Ceramics

From the released tritium (table 3), the specific and the total inventory  $I$  (per capsule) have been estimated. Together with the measured production rate  $p$  (table 2), tritium residence times referring to the corresponding irradiation temperatures have been determined according to  $\tau = I / p$ . The values are given in the table below. The residence time for the  $\text{Li}_4\text{SiO}_4$  pellets of 4 h is in reasonable agreement with the estimated inpile value of 1 h [3]. The value for the  $\text{Li}_4\text{SiO}_4$  pebbles is consistent with previous inpile results [4].

Capsule no. ceramic	1	2	5	8
Irrad. Temp. (°C)	pebbles 270 - 473	$\text{Li}_4\text{SiO}_4$ pellets 550 - 560	$\text{Li}_2\text{O}$ pellets 550 - 557	$\text{Li}_2\text{O}$ pellets 495 - 550
Spec. inventory (MBq/g)	18484	1219	70.5	72.4
Inventory/capsule (MBq)	5194	748	32	45
Meas. prod. rate / caps (MBq/h)	122	177	139	146
Residence time (h)	43	4.2	0.23	0.31

In fig. 3 and 4 sample temperature and tritium release rate of the investigated ceramics for 5 °C/min ramps are shown on a logarithmic scale as a function of time. What concern  $\text{Li}_4\text{SiO}_4$ , the release of the pebbles (fig. 3 top) with a dominant peak below 600 °C is characteristic for pure  $\text{Li}_4\text{SiO}_4$ , whereas that of the pellets (fig. 3 bottom), with a prominent peak at 700 °C is characteristic for  $\text{Li}_4\text{SiO}_4$  with carbonate impurities [10]. This is consistent with the observed large weight loss of  $w_p$  to 4.3 % and the black color after dehydration before irradiation (600 °C, 4 h, vacuum) [8] and explains the large inpile residence time of this sample at 460 °C.

Release from  $\text{Li}_2\text{O}$  is considerable faster than that of  $\text{Li}_4\text{SiO}_4$ , with a maximum at about 500 °C and only very small peaks at higher temperatures (fig. 4). This is consistent with the small residence times (see table above), which are in agreement with previous inpile tests [11].

### 4.3 Beryllium

In table 4 irradiation conditions and tritium balance data of the annealed beryllium pellets are summarized. Tritium is generated in beryllium by the following reactions:  ${}^9\text{Be}(n, t) {}^7\text{Li}$  (threshold 11.6 MeV) and  ${}^9\text{Be}(n, \alpha) {}^6\text{He}$  (threshold 0.67 MeV)  $\beta_{0.6s} \rightarrow {}^6\text{Li}(n, \alpha)t$ . The calculated production data are based on specific production values of 384, 557 and 812 MBq/g for capsule 1, 2 and 5, respectively [8].

Pellet 1 of capsule 1 was the only pellet, which was not in contact with ceramic. Therefore for this pellet, assuming that the inpile release at  $\leq 270$  °C is negligible, the measured release should be equal to the calculated production. This is not the case. The calculated production is a factor 2.6 too low (table 4), probably due to uncertainties in cross section and / or neutron spectra. Assuming that this correction factor also holds for the other pellets, corrected production values have been estimated (table 4).

In addition to the tritium generated in beryllium, a fraction of the tritium produced in the surface layer of the ceramic, is injected into those beryllium pellets, which are in contact with ceramic. Indications for this process is also provided by SEM analysis [2] (see also section 5.3.2). The amount of injected tritium has been determined numerically. First the range of the 2.74 MeV tritons from the  ${}^6\text{Li}(n, \alpha)t$  reaction in the ceramics is determined (34 and 36  $\mu\text{m}$  for 100 % dense  $\text{Li}_4\text{SiO}_4$  and  $\text{Li}_2\text{O}$ , respectively). Then the ceramic region near the interface is divided into thin, equal layers. Using the triton ranges, the fraction of injected to generated tritium can be determined for each layer by geometrical considerations. The total injected tritium (table 4) is calculated by adding these fractions and multiplying the sum by the tritium produced per layer [8]. The amount of injected tritium is several times larger than that produced in the beryllium.

From the data of table 4 the following conclusions may be drawn:

#### 1. Irradiation temperature 270 °C (capsule 1)

As mentioned, the measured inventory of pellet 1, which was not in contact with ceramic, was used to determine a correction factor for the calculated tritium production. For pellet 6, the measured inventory (719 MBq) minus the corrected production (169 MBq) amounts to 555 MBq. This inventory is assumed to be due to that fraction (83 %) of the injected tritium (666 MBq), which is not released during irradiation at 270° C.

## 2. Irradiation temperature 550° C (capsule 2 and 5)

Measured inventories are for capsule 2 (within uncertainties) equal and for capsule 5 somewhat smaller than the corrected production, indicating that essentially all of the injected and for capsule 5 even a certain fraction of the generated tritium is released during irradiation at 550° C.

To summarize, at 270° C all generated and a large fraction (83 %) of the injected tritium is stored, whereas at 550° C essentially all injected and probably also a remarkable fraction (up to 40 %) of the generated tritium is released during the 70 d-irradiation.

In fig. 5 the linear ramp and in fig. 6 the step tests with beryllium are shown. A small uncertainty in the release curves is caused by the fact, that the detector background is generally a little bit larger after than before annealing. The first annealing run of each pellet was evaluated using the background before annealing. This is the more appropriate value for the small release at low temperature at the beginning of annealing.

The three ramp curves are very similar (fig. 5). A measurable release is only observed above 600° C. Release maximum is achieved at the maximum temperature (850 °C). The similarity of release from pellet 1 of capsule 1 (fig. 5 top), which was not in contact with ceramic, with that of the other two pellets, which were in contact with ceramic, confirm the previous conclusion, that at 550 °C irradiation temperature, only the tritium generated in the beryllium is stored.

The step release curves for the two pellets irradiated at 550 °C (fig. 6, center and bottom) are again very similar. In agreement with the ramp tests, a measurable release occurs only above 600° C. The release curve of the pellet irradiated at 270 °C (fig. 6 top) is quite different:

1. a remarkable release ( $> 300$  Bq/s) is already observed at 500 °C and release rate at 850 °C drops remarkably faster than that of other pellets
2. maximum release and inventory (table 4) is much higher than for the other pellets

These observations confirm the previous conclusion based on the inventories, that this pellet contains, in addition to the generated, also injected tritium. Release of the injected tritium is evidently faster than that of the generated. This is not surprising, because the generated tritium has to move through the bulk of the high-density beryllium.

Very crude estimations of the residence time for the injected tritium from the slope of the logarithmic release of pellet 6 from capsule 1 (fig. 6 top) yield 5 h at 500 °C and  $\leq 1$  h in the region  $\geq 600$  °C. These values are consistent with the conclusion based on the inventories that at 550 °C essentially all injected tritium is released during irradiation.

Release of all other pellets, which are assumed to contain essentially only generated tritium, is very slow in the region  $\leq 600$  °C. Release behaviour during stepwise temperature increase is characterized by weak peaks, which drop quickly to release rates  $r_o < 100$  Bq/s (fig. 6, center and bottom), corresponding to the experimental uncertainty. Based on these values, the measured inventory  $I$  of about 250 MBq (table 4) and using the relation  $\tau = I/r_o$ , the residence time of the generated tritium in the region  $\leq 600$  °C is estimated to be  $> 1$  month. This value is consistent with inventory based conclusion, that at 550 °C at most a fraction of the generated tritium is released during irradiation. As mentioned, at 850 - 860 °C an average residence time of about 1 d was observed for the generated tritium.

It should be mentioned that after irradiation an oxide layer on the surfaces of the beryllium pellets of  $\leq 5$   $\mu\text{m}$  in contact with steel and  $\leq 10$   $\mu\text{m}$  in contact with ceramic is observed (section 5.3 and [2]).

In a previous PIE study of CEN Saclay [2] using the same type of beryllium pellets from other SIBELIUS capsules irradiated at 550 °C, less than 5 % of the tritium was extracted by stepwise annealing at 300 and 500 °C. This figure is in reasonable agreement with our value of about 2 % for the same temperature steps and pellets irradiated at 550 °C (pellet 15 of capsule 2 and 5, table 3).

Baldwin [12] studied tritium release from 80 % (BeO 0.9 %, grain size 25  $\mu\text{m}$  and from 100 % (BeO 1.7 %, grain size 10 - 40  $\mu\text{m}$ ) dense beryllium irradiated to fluences ( $> 1$  MeV) of  $2.6 \cdot 10^{21}$  and  $4.9 \cdot 10^{22}$   $1/\text{cm}^2$ , respectively. At 500 °C 85 % and 1 % of the tritium were released from the 80 and 100 % dense material, respectively. The figure for the 100 % dense material is consistent with the results for the 98 % dense material of this work. In addition, he observed for both materials at 600 °C a burst release of nearly the entire residual inventory. For the SIBELIUS beryllium specimens such an effect was neither observed in [2] nor in this study.

The conclusion drawn by Jones and Gibson [13] from their tritium release studies with unirradiated beryllium, that tritium is trapped at sites with a range of activation energies such that only a fraction of the tritium is released at any temperature is consistent with our observations.

## 5. Chemical compatibility of beryllium with breeder and cladding materials

### 5.1 Samples

From the capsules KfK 02 and KfK 05, samples were selected for examination that are marked with "Dienst" in Fig. 7 and 8. These samples had been irradiated at 550 °C. Samples from capsule KfK 01A can be disregarded because they did not show any relevant change in microstructure after irradiation at 270°C.

The selected samples offered contact faces of beryllium (KfK 02-11 and 13, KfK 05-11 and 13) with  $\text{Li}_4\text{SiO}_4$  (KfK 02-12),  $\text{Li}_2\text{O}$  (KfK 05-12), austenitic 17 % Cr- 13 % Ni steel 316 L (KfK 02-10, KfK 05-10) and martensitic-ferritic 10,5% Cr steel 1.4914 (KfK 02-14, KfK 05-14). The sample faces belonging to the different couples can be identified in the top parts of Fig. 7 and 8; the faces are marked S1 or S2 each.

Axial sections of the cylindrical sample discs are prepared for the microscopic examination of chemical reactions on the contact faces. The sample faces examined were mostly polished, but also etched on the cladding steels and contrasted on the breeder materials.

It is to be mentioned before, that only the beryllium samples in contact with breeder materials showed important microstructure changes.

### 5.2 Relevant results of previous annealing tests

In 600°C annealing tests up to 1000 h no discernable reaction of beryllium could be found with  $\text{Li}_2\text{O}$  [14] and  $\text{Li}_2\text{SiO}_3$  [15]. A rough extrapolation of  $\text{Li}_4\text{SiO}_4$  results obtained at higher temperatures for the conditions of the present irradiation (1690 h, 550 °C) results in a rather thin reaction layer consuming  $< 5 \mu\text{m}$  Be. At higher annealing temperatures  $\geq 650^\circ\text{C}$  a beryllium oxide layer was observed on the interface (Fig. 9) which can also contain multinary Be-Li-Si oxide [16].

Considerable chemical reaction of beryllium with steel 316 L was already observed at 600°C [17, 18]. A beryllium diffusion zone with BeNi precipitates penetrated into the steel (Fig. 10) and cavities formed on the beryllium surface. Correlations were formulated for the reaction zone growth [15, 19] which predict a steel penetration depth of about 15  $\mu\text{m}$  after 1690 h at 550°C (like in the present experiment). Since the atom fraction of Be in the diffusion zone probably exceeds that of Ni only by the Be solubility in Fe ( $< 10$  at %) the corresponding consumption of Be amounts to a few  $\mu\text{m}$ .

The beryllium reaction with steel 1.4914 was much weaker and not yet detectable after 1500 h at 600°C [18, 19].

### 5.3 Post-irradiation examination results

#### 5.3.1 Beryllium with steel

As expected, only minor chemical reactions were observed on the beryllium / steel couples after irradiation at 550°C. Cr-Ni steel 316 L in the polished condition shows a reaction product layer of 2 - 3  $\mu\text{m}$  thickness which becomes more distinct after etching, together with precipitates mainly in deformation zones to 15  $\mu\text{m}$  depth (Fig. 11a -c). Intermetallic Be-Fe-Ni layers on the steel surface had also been found after annealing tests [18]. The precipitates probably consist of BeNi. The corresponding beryllium consumption caused considerable roughening of a maximum depth of 3 - 4  $\mu\text{m}$  on the beryllium surface (Fig. 12a, b).

As already observed in annealing tests [18, 19] the reaction extent is smaller with Cr steel 1.4914, but not in the large ratio found at higher temperatures. The depth of surface roughening is comparable with that on etched 316 L samples (max. 3 - 4  $\mu\text{m}$ , Fig. 13a, b). A diffusion zone with very fine precipitates seems to be about 10  $\mu\text{m}$  in depth. The roughening depth of the beryllium surface in contact with steel 1.4914 appears considerably smaller than with 316L ( $\sim 1$   $\mu\text{m}$ , Fig. 12c). So BeNi formation seems to be mainly responsible for the beryllium consumption also at 550°C.

In any case it has been shown that the correlations describing the reaction rate of beryllium with the steels 316L and 1.4914 in annealing tests remain virtually valid also under neutron irradiation. This is not surprising, because it is well-known that the thermal diffusion rate at  $T \approx 0,5 T_m$  (in K) exceeds that of irradiation-induced diffusion by orders of magnitude. It is of minor technical importance whether some reduction of the chemical attack can be also due to a beryllium oxide layer generated by tritium water from the breeder burnup or by water impurity of the breeder materials [2]. The KfK observations gave no relevant indications.

#### 5.3.2 Beryllium with breeder materials

At the interfaces between Be discs and  $\text{Li}_2\text{O}$  or  $\text{Li}_4\text{SiO}_4$  pellets no indications of a chemical reaction were observed after irradiation at 550°C, except a slight roughening of the beryllium surface (max. 2  $\mu\text{m}$ , Fig. 16, 17). The microstructure of the breeder materials near the contact face appeared unchanged in comparison with that in the sample interior (Fig. 14, 15). It seems that the temperature-dependent decrease of the Be/ $\text{Li}_4\text{SiO}_4$  reaction rate in the range of  $T \approx 650$  °C was even underestimated on the basis of annealing test results [15].

So the analyzing efforts concentrated on a new phenomenon which is certainly caused by irradiation effects. Rather large pores (2 - 15  $\mu\text{m}$  diam. ) were observed in a zone of about 40  $\mu\text{m}$  depth at the beryllium surface (Fig. 16 to 19). The pores grew larger at the interface with  $\text{Li}_2\text{O}$  than with  $\text{Li}_4\text{SiO}_4$ . Similar pore formation was found in CEA investigations on  $\text{Be}/\text{Li}_2\text{ZrO}_3$  and  $\text{Be}/\text{LiAlO}_2$  couples of the SIBELIUS experiment [2].

As discussed earlier, there is a specific irradiation effect on the beryllium samples in contact with breeder materials that results from the bombardment with high-energy tritons and  $\alpha$ -particles generated in the breeding reaction  ${}^6\text{Li} (n, \alpha)\text{t} + 4.7$  MeV. The penetration depth of 2.7 MeV tritons or 2.0 MeV  $\alpha$ -particles in beryllium of theoretical density amounts to about 40  $\mu\text{m}$  or 7  $\mu\text{m}$  [20]. Therefore it seems probable that the observed pore formation is caused by triton bombardment. This confirms the conclusion from the tritium release experiments with beryllium.

From the values of table 2 the total lithium burnup is determined to be about 2 and 1 % and the specific tritium production correspondingly about 1 and 0.5 at % for  $\text{Li}_4\text{SiO}_4$  (capsule 2) and  $\text{Li}_2\text{O}$  (capsule 5), respectively (the  ${}^6\text{Li}$  enrichment of  $\text{Li}_2\text{O}$  is only 2 %, see table 1). From these figures, the triton ranges ( $\approx 40 \mu$  for both, ceramics and beryllium) and the calculated fraction of injected to produced tritium of about 20 % (see section 4.3), the concentration of injected tritium in the surface layer of beryllium is about 0.2 and 0.1 at % for  $\text{Li}_4\text{SiO}_4$  and  $\text{Li}_2\text{O}$ , respectively. If the pores were equilibrium gas bubbles with an internal pressure  $p = 2 \gamma / r$  (surface energy  $\gamma \approx 1\text{J}/\text{m}^2$ ) the gas pressure at room temperature is about  $p = 0.5 - 3$  bar. As the pore volume fraction observable in Fig. 16 - 19 amounts to some percent, the resulting  $\text{T}_2$  gas content is in the order of  $10^{-5}$  T atom/Be atom in the bombarded zone of 40  $\mu\text{m}$  depth. Accordingly, the bubble formation would only require about 1% of the injected tritium. Bubble nucleation and growth is enhanced by vacancy formation in the atom collision cascades produced by the tritons and also by fast neutrons.

It is to be added that very fine precipitates and/or pores were observed in the irradiated beryllium samples, may be  $\text{BeO}$  particles precipitated from supersaturated solid solution under irradiation (specified oxygen content  $< 300$  appm, solubility probably far below 100 appm [21]) or helium bubbles (He content in the order of 100 appm from the  ${}^9\text{Be} (n, \alpha) {}^6\text{He}$  reaction [22]). This microstructure constituent generally disappeared near the beryllium surface. So there is no reason to suppose a connection with the coarse bubble formation discussed above.

## 6. Conclusions

In agreement with previous studies, it was found that the release of tritium generated in beryllium is very slow. For beryllium which is in contact with breeder ceramic during irradiation, a second type of tritium inventory is observed. This inventory is caused by injection of the 2.7 MeV tritons generated in the ceramic and may be several times larger than that generated in the beryllium. Although release of injected tritium is faster than that of the generated, it is to be expected, that for typical blanket temperatures of about 400 °C, a remarkable fraction of the injected and essentially all of the generated tritium is stored in beryllium. Therefore, although the tritium production rate of the ceramic is about three orders of magnitude larger than that of beryllium, the tritium inventory of beryllium may be comparable or even exceed that of the ceramic. For safety and reasons of economics, the tritium inventory in the blanket should be small. Therefore tritium release of beryllium is an aspect of growing importance in fusion blanket design.

From the compatibility studies the main conclusions are:

- The chemical reaction of beryllium with steel cladding is sufficiently described by the results of laboratory annealing tests also for the behaviour under neutron irradiation.
- The same probably holds for the chemical reactions of beryllium with breeder materials.
- In beryllium which was in contact with ceramic, pores are observed in the surface layer of beryllium over a thickness corresponding to the range of the 2.7 MeV tritons from the  ${}^6\text{Li} (n, \alpha)\text{t}$  reaction. This direct evidence of triton injection from the ceramic confirms the conclusions from the tritium release investigations of beryllium.

## Acknowledgements

The authors thank E. Kaiser and F. Weiser from the hot cells for the extensive microstructure investigations and T. Eberle and J. Lebkücher for performing and evaluating the tritium annealing experiments.

This work was performed in the framework of the KfK Nuclear Fusion Project and is supported by the European Communities within the European Fusion Technology Program.

## References

- [1] N. Roux, H. Briec, M. Bruet, T. Flament, C. Johnson, M. Masson, A. Terlain, F. Tournebize, *J. Nucl. Mater.* 179 - 181 (1991) 827
- [2] N. Roux, J.J. Abassin, M. Briec, D. Cruz, T. Flament, I. Schuster, "Compatibility Behaviour of Beryllium with  $\text{LiAlO}_2$  and  $\text{Li}_2\text{ZrO}_3$  Ceramics, with 316L and 1.4914 Steels in SIBELIUS", 5th Int. Conf. on Fusion Reactor Materials (ICFRM-5), Clearwater, Fla, Nov. 17 - 22, 1991, paper PA 22
- [3] M. Briec, "The SIBELIUS Experiment", CEN Grenoble, Note Technique DTP/SECC/90/90, December 6, 1990
- [4] H. Werle, W. Breitung, M. Briec, R.G. Clemmer, H. Elbel, H.E. Häfner, M. Masson, G. Schumacher, H. Wedemeyer, *J. Nucl. Mater.* 155 - 157 (1989) 538
- [5] W. Breitung, M. Briec and H. Werle, *Fusion Eng. Design* 8 (1989) 323.
- [6] H. Wedemeyer, E. Günther, unpublished report, Nov. 1989
- [7] H.-J. Ritzhaupt-Kleissl, W. Laub, Chr. Odemer, unpublished report, December 1989
- [8] N. Roux, CEN Saclay, private communication
- [9] W. Breitung, H. Elbel, J. Lebkücher, G. Schumacher, H. Werle, *J. Nucl. Mater.* 155 - 157 (1988) 507
- [10] W. Breitung, H. Werle, W. Krug, "Tritium Release from Lithium Orthosilicate and Metazirconate: Influence of Purge Gas Additives and Sample Impurities, Order of Release Reaction", Proc. Third Specialist's Workshop on Modeling Tritium Behaviour in Ceramic Fusion Blankets, KfK, June 10 - 11, 1991 (H. Werle, ed.), p.49
- [11] M. Briec, J.J. Abassin, J.E. Johnson, M. Masson, N. Roux, H. Watanabe, in: Proc. 15th SOFT, Fusion Technology 1988, Elsevier, Amsterdam (1989), p. 1105
- [12] D.L. Baldwin, "Comparison of Results of Tritium and Helium Behaviour in Irradiated Beryllium", Beryllium Technology Workshop, Clearwater, Fla, Nov. 20, 1991 (G.R. Longhurst, INEL, ed.)
- [13] P.M.S. Jones, R. Gibson, *J. Nucl. Mater.* 21 (1967) 353
- [14] N. Sakamoto, H. Kawamura, E. Ishitsuka, Y. Ichihashi, "Compatibility test of

Be with Li<sub>2</sub>O. - Diffusion couple test", Fifth Int. Conf. on Fusion Reactor Materials, November 17 - 22, 1991, Clearwater, Florida, Paper PA 21

- [15] P. Hofmann, W. Dienst, "Chemical interactions of beryllium with lithium-based oxides and stainless steel", J. Nucl. Mater. 171 (1990) 203 - 214
- [16] O. Götzmann, unpublished report, Januar 1988
- [17] P. Hofmann, W. Dienst, "Compatibility studies of metallic materials with lithium-based oxides", J. Nucl. Mater. 155 - 157 (1988) 485 - 490
- [18] T. Flament, P. Fauvet, J. Sannier, "Compatibility of stainless steels and lithiated ceramics with beryllium", J. Nucl. Mater. 155 - 157 (1988) 496 - 499
- [19] M. Broc, T. Flament, A. Terlain, J. Sannier, "Compatibility problems in tritium breeding blankets", J. Nucl. Mater. 179 - 181 (1991) 820 - 823
- [20] A. Möslang, KfK, personal communication, 1992
- [21] H. A. Wried, "The beryllium-oxygen system" in: Phase Diagrams of Binary Beryllium Alloys, H. Okamoto, L. E. Tanner (Eds.), ASM International, Metals Park, Ohio, 1987, S. 146 - 152
- [22] M. C. Billone, R. G. Macaulay-Newcombe, unpublished report, June 1991

Tab. 1 Material properties of investigated ceramics

Pellets: 8 mm  $\varnothing$  \* 1.5 mm

Li<sub>4</sub>SiO<sub>4</sub> pebbles - type Schott 86 (KfK) 0.45 - 0.56 mm  $\varnothing$   
tempered 100 °C, 2 h, in air

- bed 8 mm  $\varnothing$  \* 4 mm

Material Type	Li <sub>4</sub> SiO <sub>4</sub> pebbles [4, 5]	Li <sub>4</sub> SiO <sub>4</sub> pellets [6, 7]	Li <sub>2</sub> O pellets [3]
Source	KfK	KfK	US
<sup>6</sup> Li enrichment (%)	7.5	7.5	2
TD (%)	93	90	80
Open / Total porosity (%)	≈ 100	≈ 70	--
Pore diameter (μm)	≤ 16	< 0.1	--
Grain size (μm)	20 - 50	≈ 50	≈ 20
Specific surface (m <sup>2</sup> /g)	5.9	--	--

Table 2 Irradiation conditions

	Caps. no. Ceramic		1 Li <sub>4</sub> SiO <sub>4</sub> pebbles	2 Li <sub>4</sub> SiO <sub>4</sub> pellets	5	8 Li <sub>2</sub> O pellets	
Production	Ceramic	Tritium meas. [3]	(mC/d/caps.)	79	115	90	95
			(10 <sup>20</sup> T/caps.)	1.15	1.68	1.31	--
	Ceramic	Tritium calc[8]	(10 <sup>20</sup> T/cm <sup>3</sup> )	4.86 - 5.30	9.44	5.02	--
			(10 <sup>20</sup> T/caps.)	1.0	2.8	1.5	--
		<sup>6</sup> Li burnup calc. (%)	24	29	41	--	
	Beryllium calc. [8]	Tritium (10 <sup>8</sup> Bq/g)	3.84	5.57	8.12	--	
		<sup>4</sup> He (mm <sup>3</sup> /g)	249	329	355	--	
Heating calc. (W/cm <sup>3</sup> )	Neutron	Ceramic [8]	64	118	--	--	
	Gamma	Ceramic [8]	4.4	9	--	--	
		Steel [3]	←-----→		46	-----→	
		Beryllium [3]	←-----→		10	-----→	
Temperature	Be/steel interface <sup>c</sup>		280	550	--	--	
	Be/ceramic interface ≅ ceramic min.		270 <sup>c</sup>	550 <sup>m</sup>	550 <sup>m</sup>	--	
	Ceramic max. <sup>m</sup>		473	--	--	550	
	Ceramic ΔT <sub>max</sub> <sup>c</sup>		200 <sup>c</sup>	10 <sup>c</sup>	7 <sup>c</sup>	55 <sup>c</sup>	

<sup>m</sup> measured, <sup>c</sup> calculated

Table 3 Tritium annealing results  
Purge gas He + 0.1 % H<sub>2</sub>, 50 standard-cm<sup>3</sup>/min

Caps. no.	Material pellet no.	Anneal. date	Mass (g)	Heating	Release (MBq)	End anneal.		Total inv. (MBq)
						Rel rate (Bq/s)	Inv. (MBq)	
1	Be 1	Aug 19, 91	0.1890	Ramp	149	110	10	191
		Aug 20, 91		Step 850 °C (4 h)	7			
		Sept. 91		Steps 860 °C (31 h)	25			
	Be 6	Aug 21, 91	0.1711	Step 300, 400, 500°C	21	800	69	719
		Aug 22, 91		Step 600, 850 °C	629			
2	Be 9	Aug 27, 91	0.1877	Ramp	178	500	43	238
		Aug 28, 91		Step 850 °C (6 h)	17			
	Be 15	Oct 11, 91	0.1761	Step 300, 400, 500°C	5	500	43	244
		Oct 14, 91		Step 600, 850 °C	182			
		Oct 15, 91		Step 850 (6 h)	14			
5	Be 9	Oct 17, 91	0.1868	Ramp	142	700	60	229
		Oct 18, 91		Step 850 °C (6 h)	27			
	Be 15	Nov 28, 91	0.1720	Step 300, 400, 500°C	5	800	69	271
		Nov 29, 91		Step 600, 850 °C	175			
		Dec 2, 91		Step 850 °C (5 h)	22			
1	Li <sub>4</sub> SiO <sub>4</sub> pebbles sample 1	Jan 14, 92	0.1037	Ramp 408 °C	742	--	--	1867
		Jan 15, 92		Ramp 509 °C	920			
		Jan 20, 92		Ramp 850 °C	205			
	sample 2	Jan 22, 92	0.1120	Ramp	2120	--	--	2120
2	Li <sub>4</sub> SiO <sub>4</sub> 16	Dec 11, 91	0.1534	Ramp	187	--	--	187
5	Li <sub>2</sub> O 16	Dec 13, 91	0.1135	Ramp	8.0	--	--	8.0
8	Li <sub>2</sub> O 4	Dec 18, 91	0.1510	Ramp	9.4	--	--	9.4
		Jan 9, 92		Step 300, 400, 500°C	10.9			
		Jan 10, 92		Step 600, 850 °C	2.3	--	--	13.2

Ramp: 5 °C / min; if not specified, max. temp. 850 °C for 3 h  
Step: if not specified 2 h

Weight losses during annealing: Be ≈ 0.05 %  
Li<sub>4</sub>SiO<sub>4</sub> pebbles 1-3 %  
Li<sub>4</sub>SiO<sub>4</sub> pellets ≈ 1 %  
Li<sub>2</sub>O ≈ 1 %

Table 4 Irradiation conditions and tritium inventory, production and injection in beryllium pellets

Capsule No.	no.	Mass (g)	Be pellets Irr. temp. (°C)	Contact	Tritium Inventory / pellet (MBq)			
					Meas. invent.	Production Calc.[8]	Corr.	Calc. injected
1	1	0.1890	≤ 270	Steel	191 ± 10	73	190	0
	6	0.1711	270	Li <sub>4</sub> SiO <sub>4</sub>	719	65	169	666
2	9	0.1877	550	Li <sub>4</sub> SiO <sub>4</sub> /steel	238	105	273	792
	15	0.1761	550	Li <sub>4</sub> SiO <sub>4</sub> /steel	244	98	255	792
5	9	0.1868	550	Li <sub>2</sub> O/steel	229	152	395	503
	15	0.1720	550	Li <sub>2</sub> O/steel	271	140	364	503

DISTRIBUTION OF SPECIMENS FOR P.I.E.

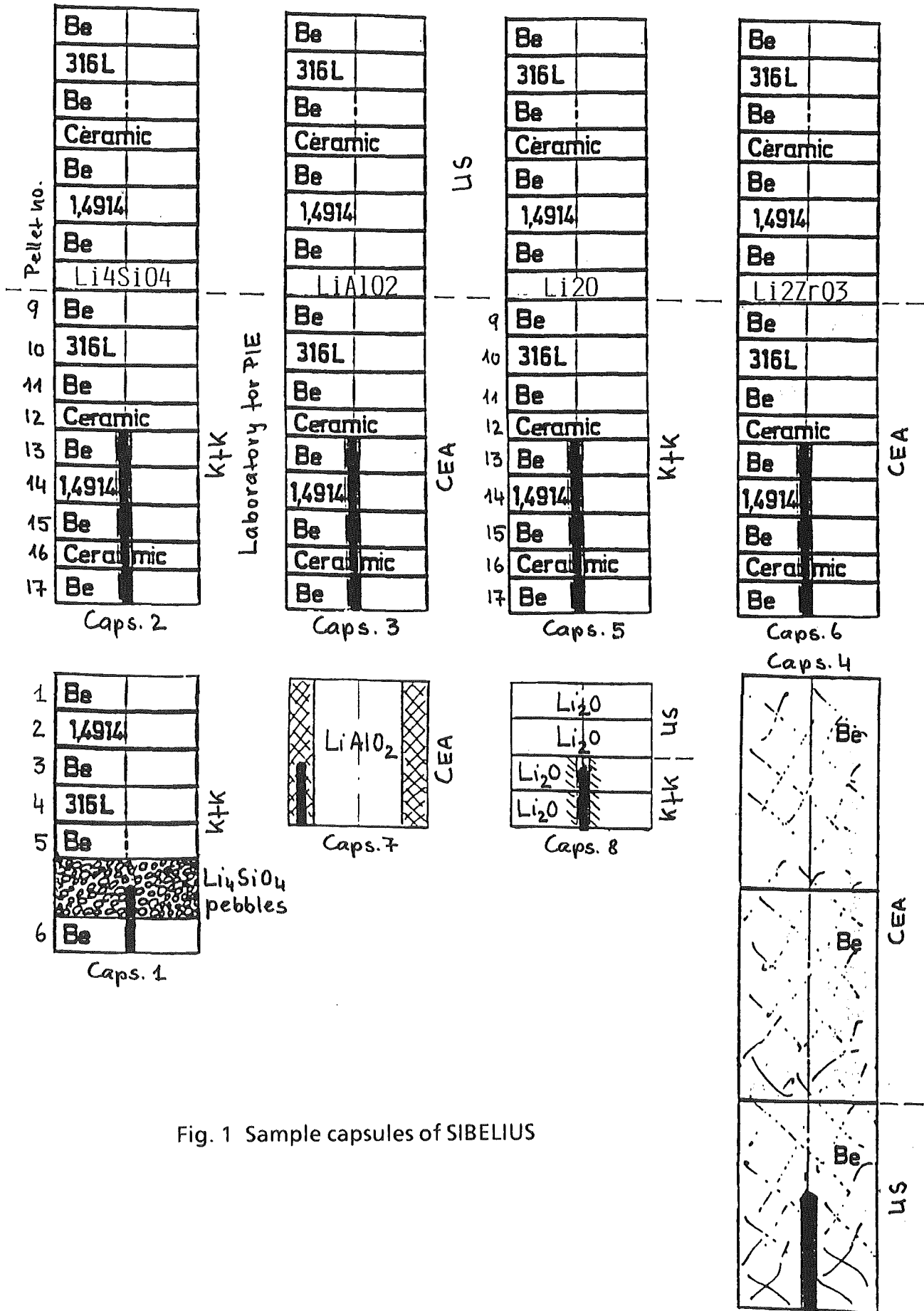
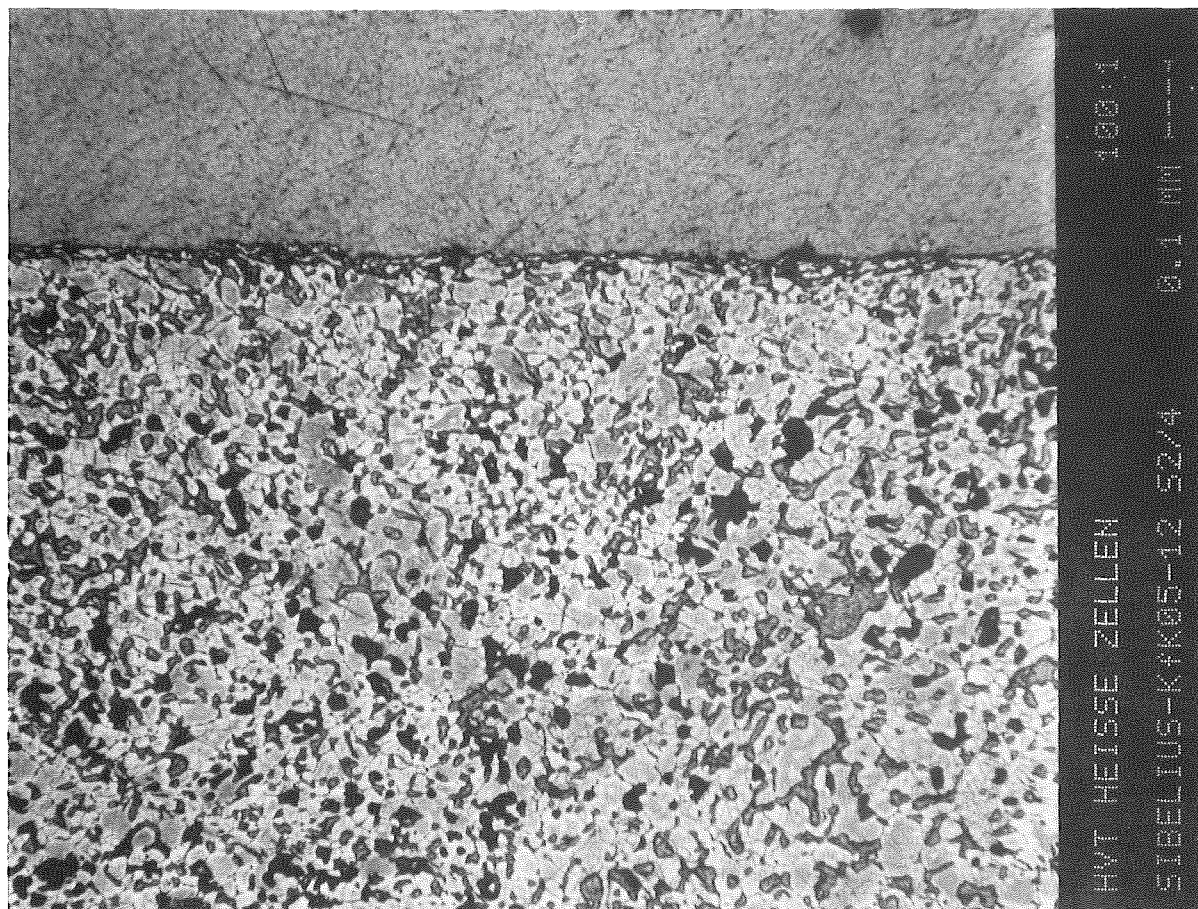
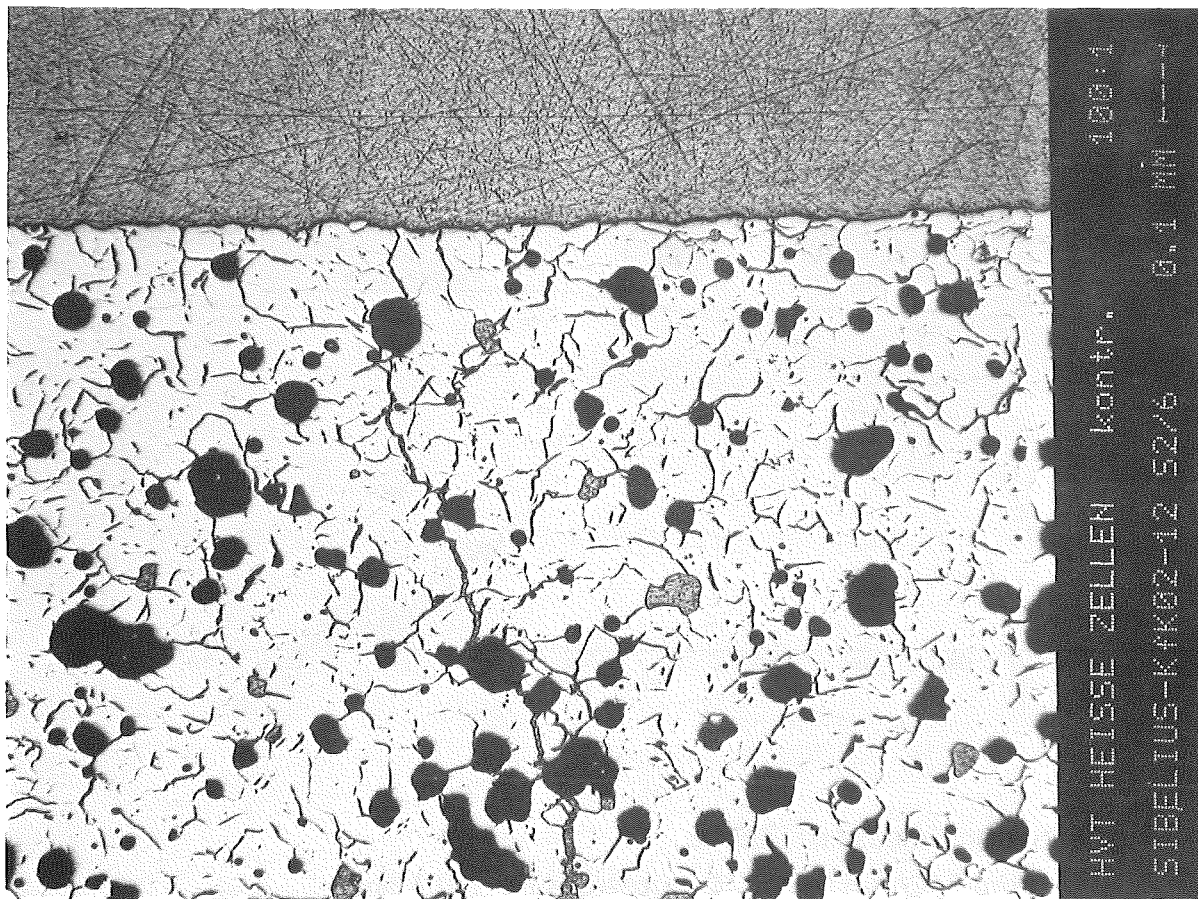


Fig. 1 Sample capsules of SIBELIUS



Li<sub>2</sub>O



Li<sub>4</sub>SiO<sub>4</sub>

Fig 2: Micrograph of Li<sub>4</sub>SiO<sub>4</sub> and Li<sub>2</sub>O pellets after irradiation

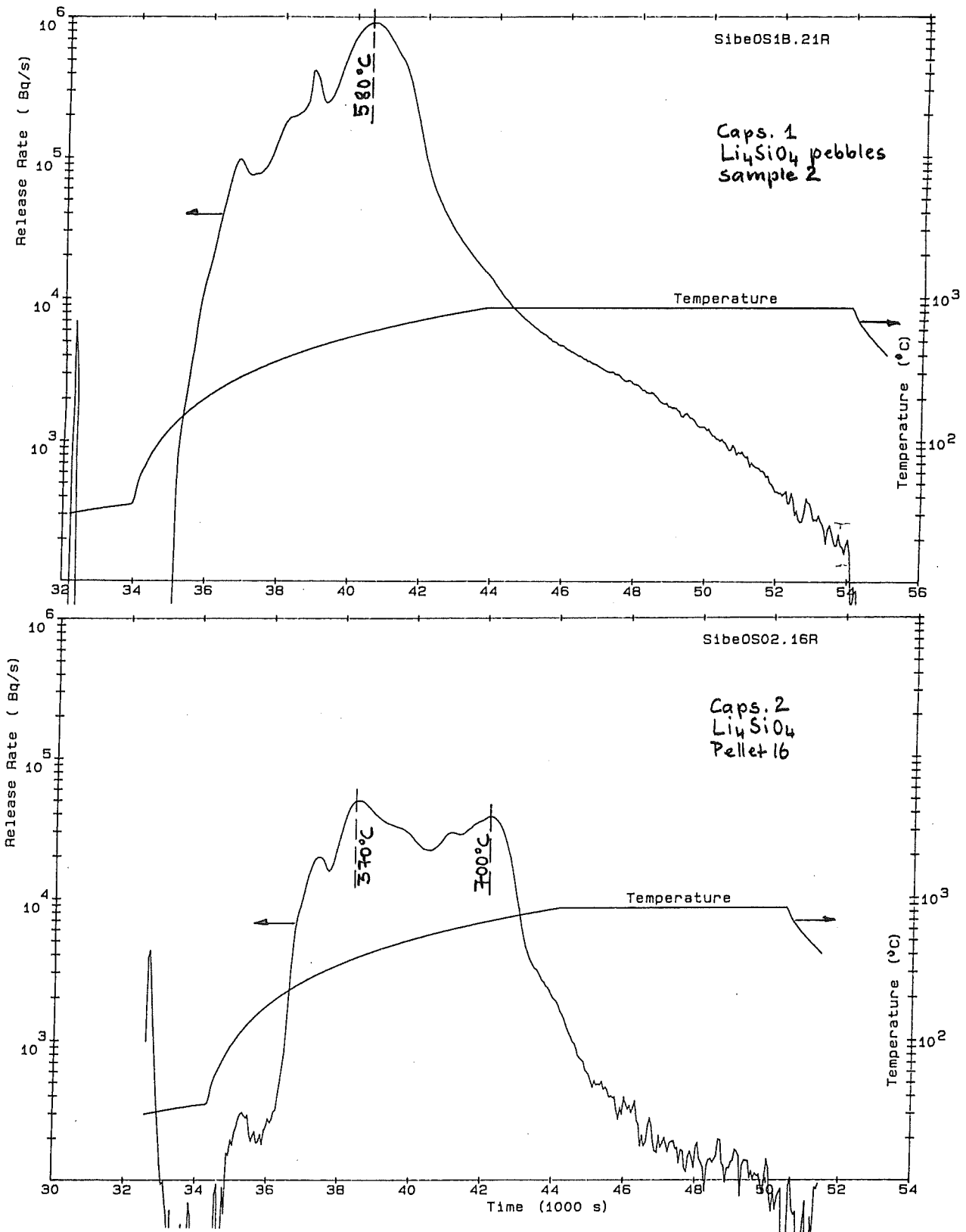


Fig. 3 Tritium release of Li<sub>4</sub>SiO<sub>4</sub>.

Ramp 5 °C/min to 850 °C, purge gas He + 0.1 % H<sub>2</sub>

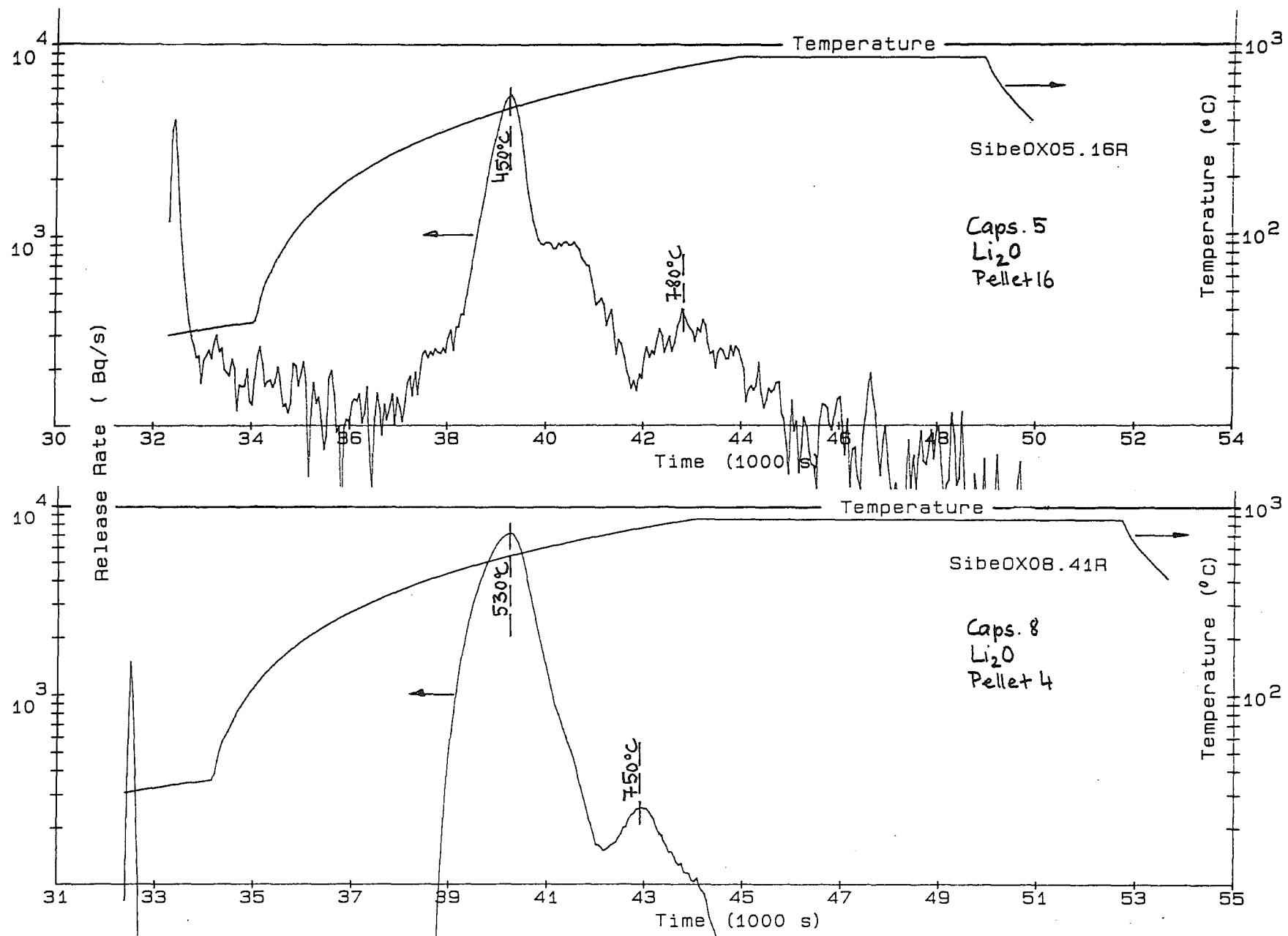


Fig.4 Tritium release of Li<sub>2</sub>O.

Ramp 5 °C/min to 850 °C, purge gas He + 0.1 % H<sub>2</sub>

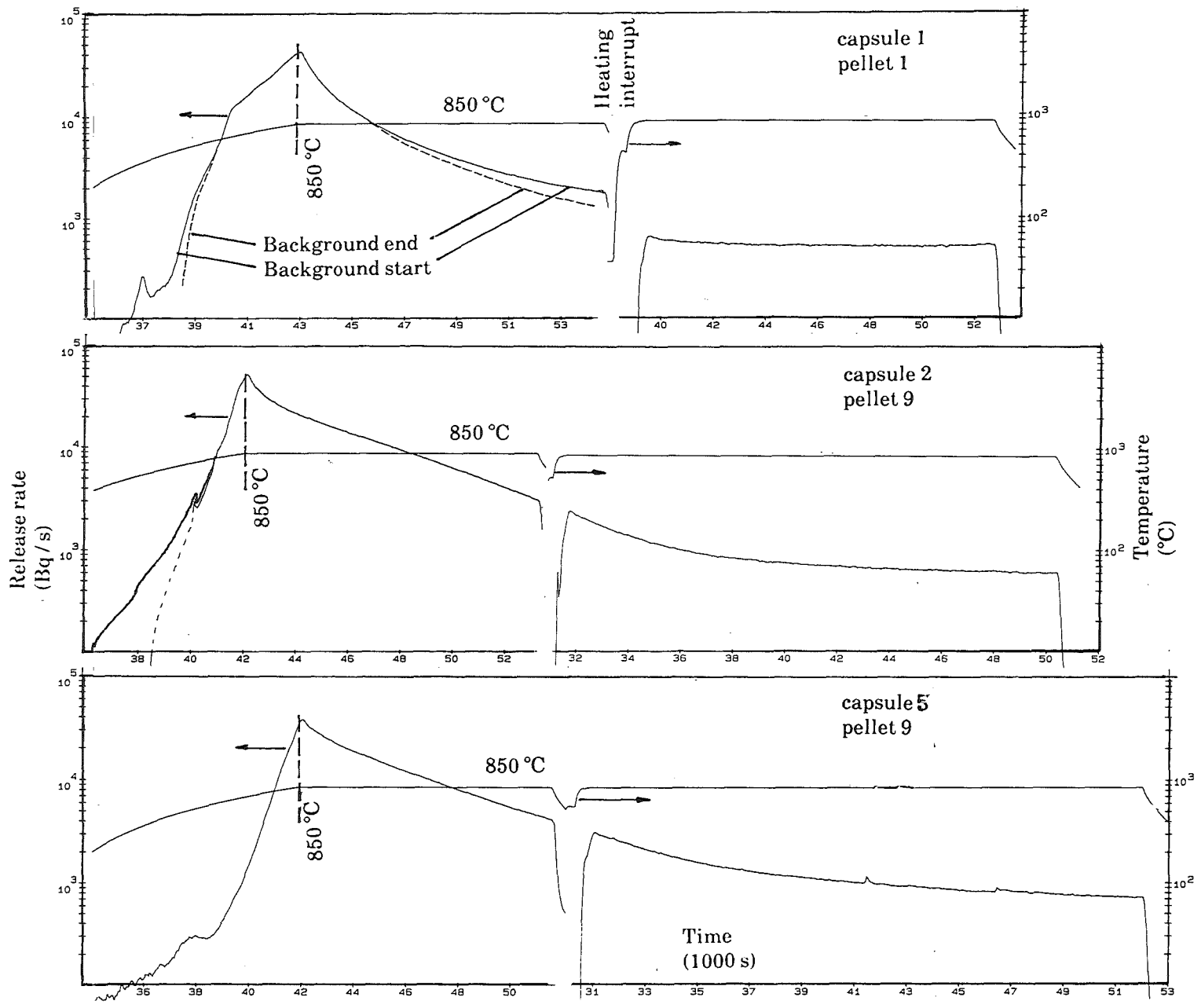


Fig. 5 Tritium release of beryllium.  
 Ramp 5 °C/min to 850 °C, purge gas He + 0.1 % H<sub>2</sub>

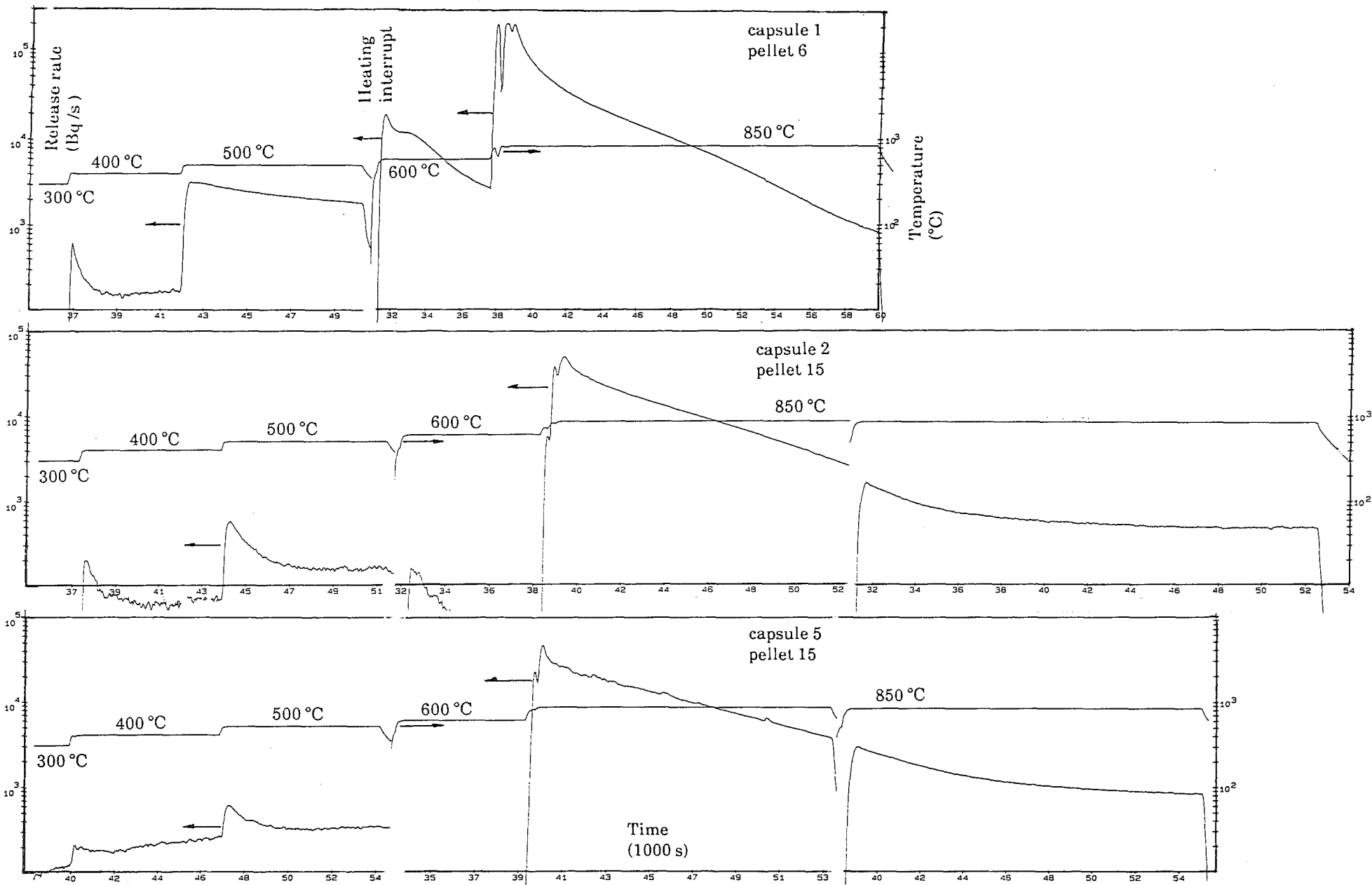
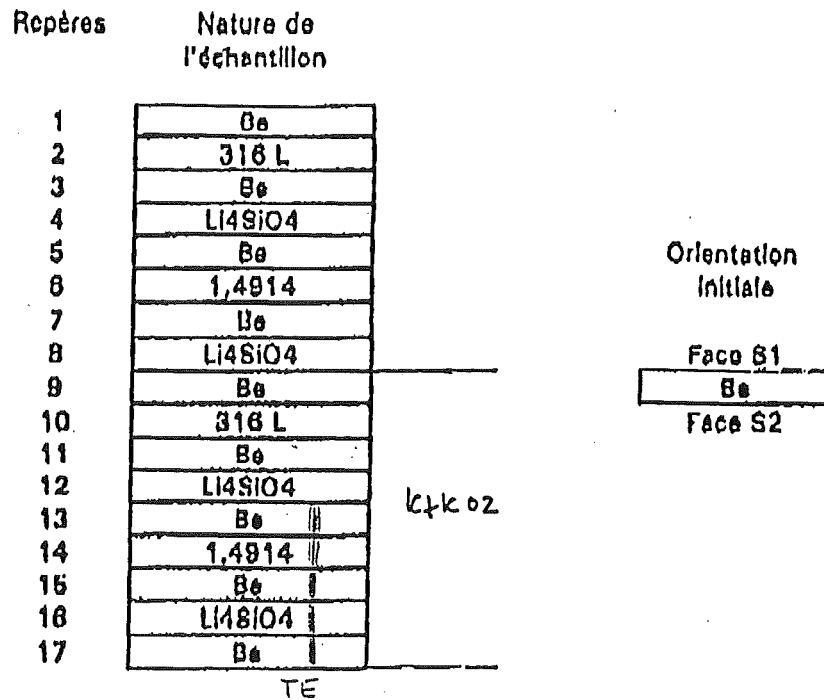


Fig. 6 Tritium release of beryllium.  
 Temperature steps, purge gas He + 0.1 % H<sub>2</sub>

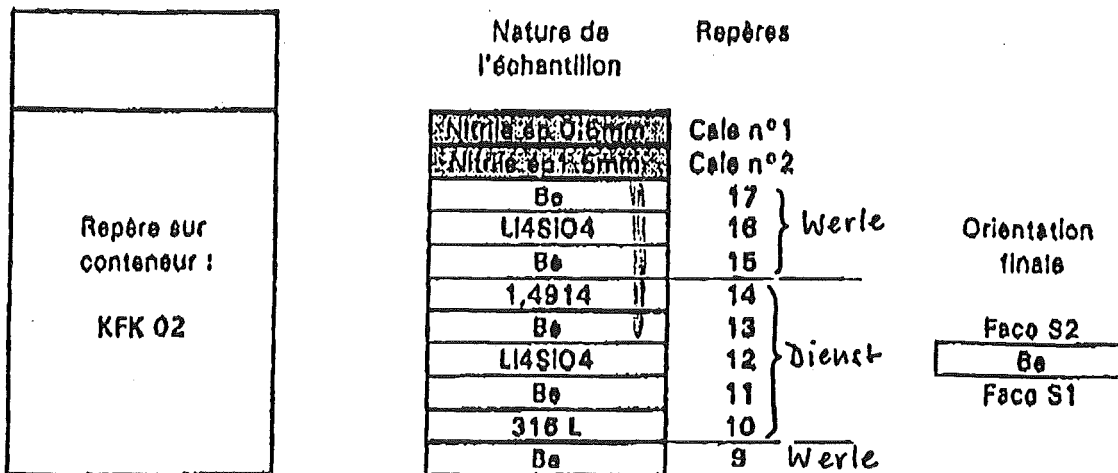
CONDITIONNEMENT DES ECHANTILLONS  
A DESTINATION DE K.F.K.

CAPSULE N°2

PLAN DE CHARGEMENT INITIAL DE LA CAPSULE



PLAN DE CHARGEMENT DU CONTENEUR



Observations :

Pastille n°2 fendue au moment de la dépose au fond du conteneur , mais sortie intègre de la capsule

Fig. 7: Arrangement of the KfK 02 samples

CONDITIONNEMENT DES ECHANTILLONS  
A DESTINATION DE K.F.K

CAPSULE N°5

PLAN DE CHARGEMENT INITIAL DE LA CAPSULE

Repères	Nature de l'échantillon	
1	Be	
2	310 L	
3	Be	
4	L120	
5	Be	
6	1,4914	
7	Be	
8	L120	
9	Be	
10	316 L	
11	Be	
12	L120	
13	Be	KFK 05
14	1,4914	
15	Be	
16	L120	
17	Be	

Orientation initiale

Face S1
Be
Face S2

PLAN DE CHARGEMENT DU CONTENEUR

Repère sur  
conteneur :

KFK 05  
05

Nature de l'échantillon	Repères	
Nitrile ép. 0,6mm	Cale n°1	
Nitrile ép. 1,5mm	Cale n°2	
Be	17	Werle
L120	16	
Be	15	
1,4914	14	Dienst
Be	13	
L120	12	
Be	11	Werle
316 L	10	
Be	9	

Orientation finale

Face S2
Be
Face S1

Fig. 8: Arrangement of the Kfk 05 samples

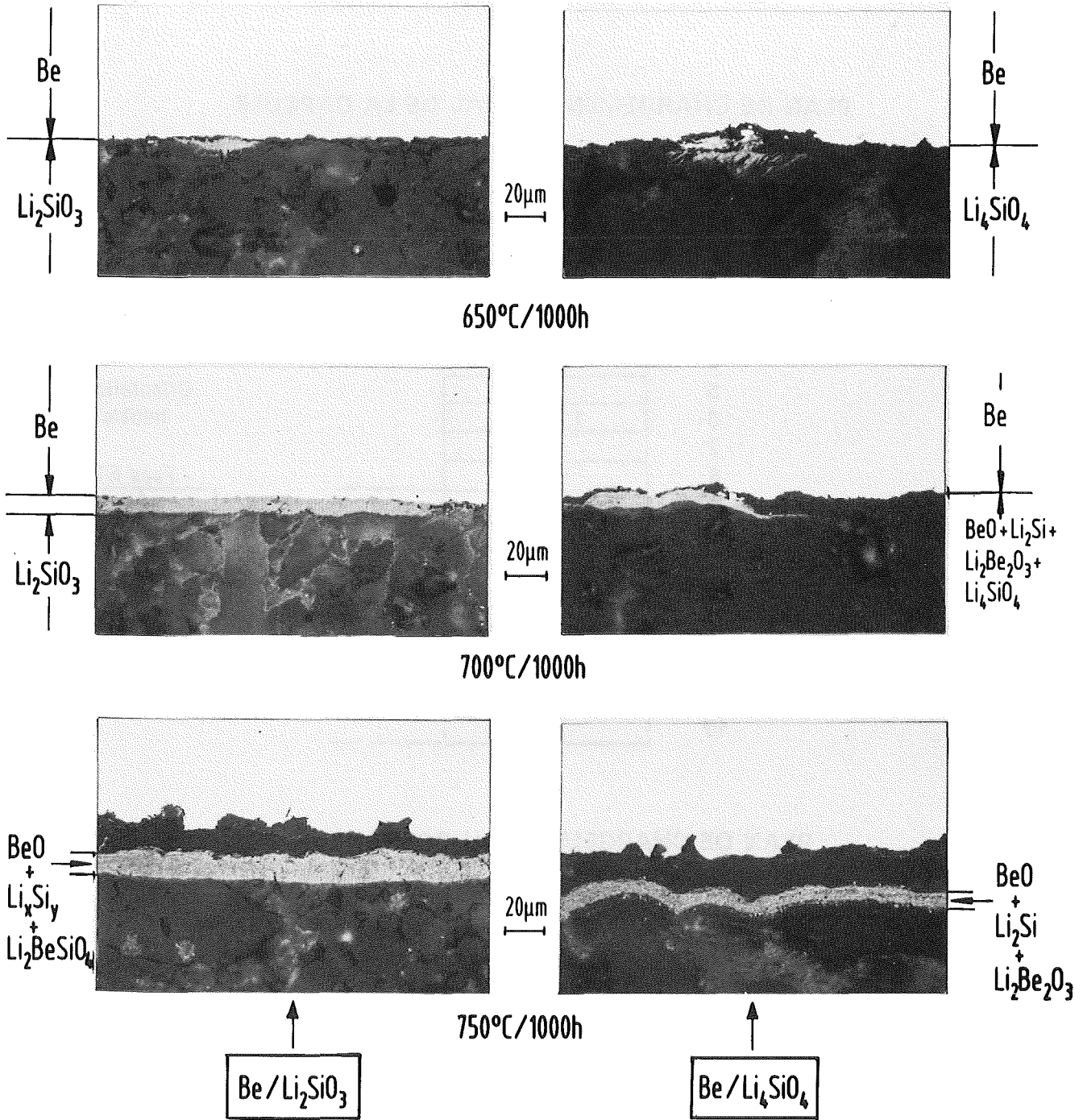


Fig.9: Reaction zones of beryllium with Li<sub>2</sub>SiO<sub>3</sub> and Li<sub>4</sub>SiO<sub>4</sub> after 1000 h at 650 to 750°C

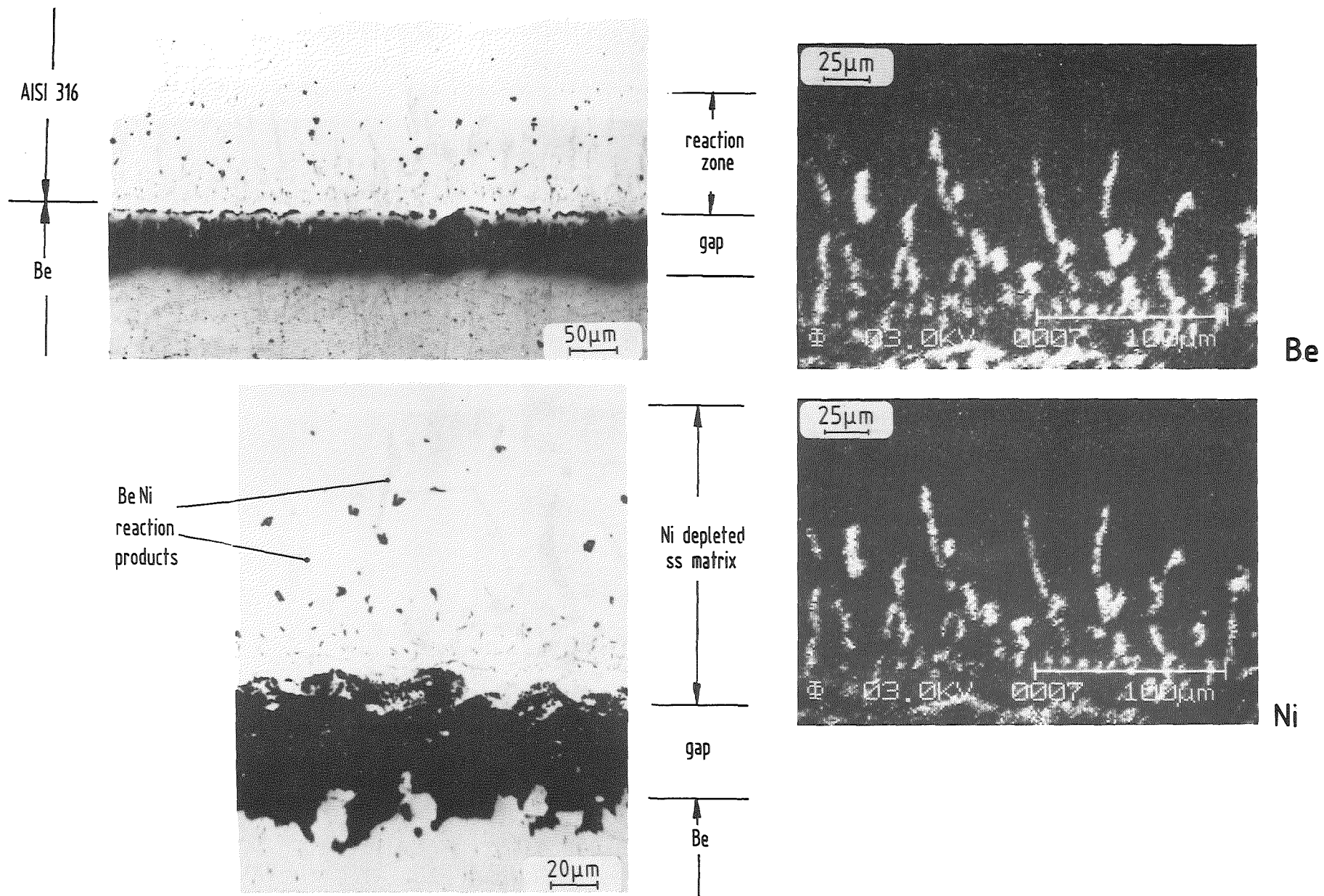


Fig. 10: Reaction zone of steel 316L in contact with beryllium after 100 h at 900°C and Be-Ni distribution picture from Auger-electron microprobe examination

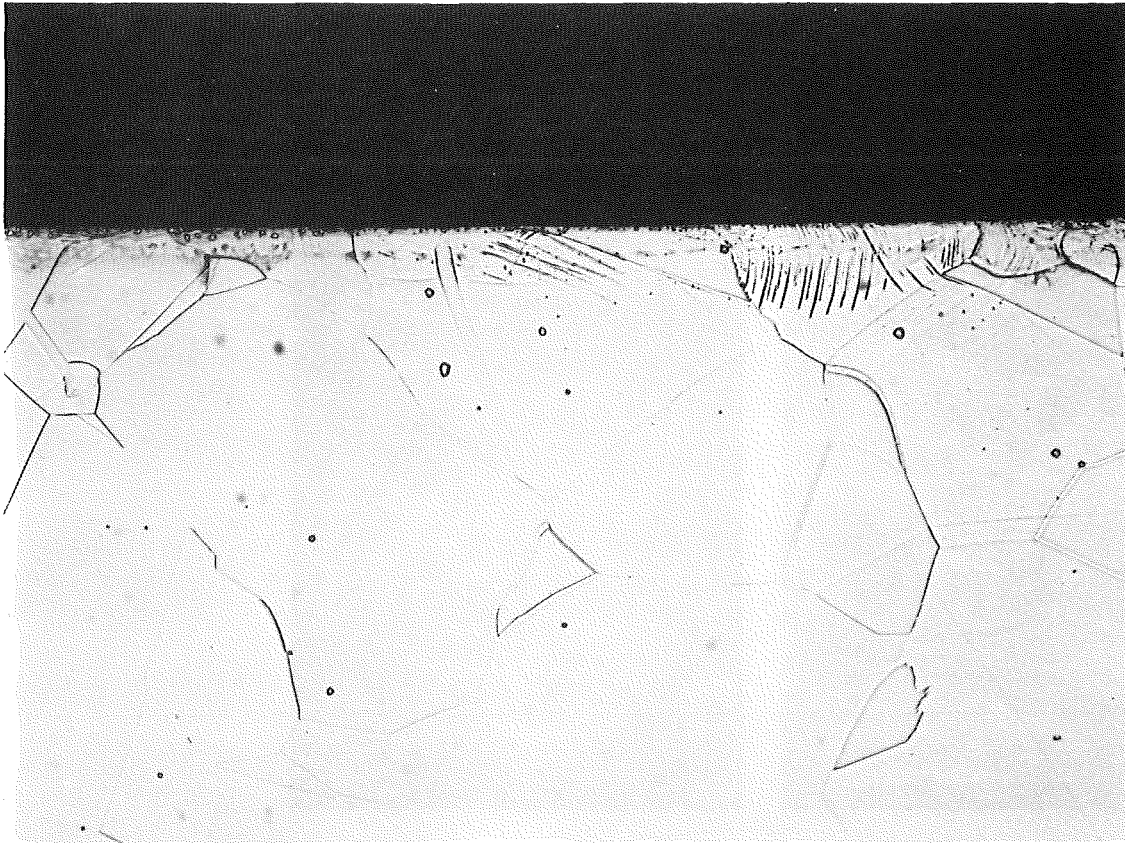


Fig. 11a: Microstructure near the surface of unirradiated steel 316 L, etched, magnif. 500x

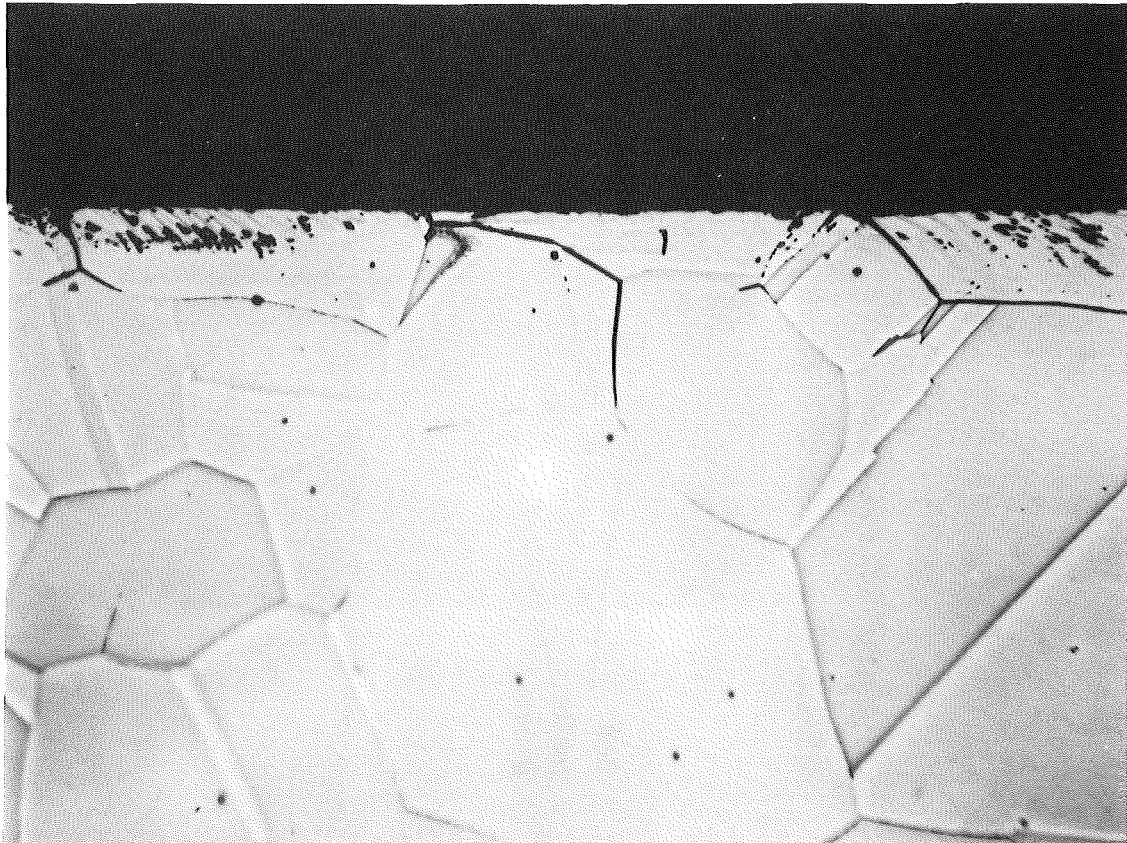


Fig. 11b: Reaction zone in the 316 L sample KfK 02-10, etched, magnif. 500 x

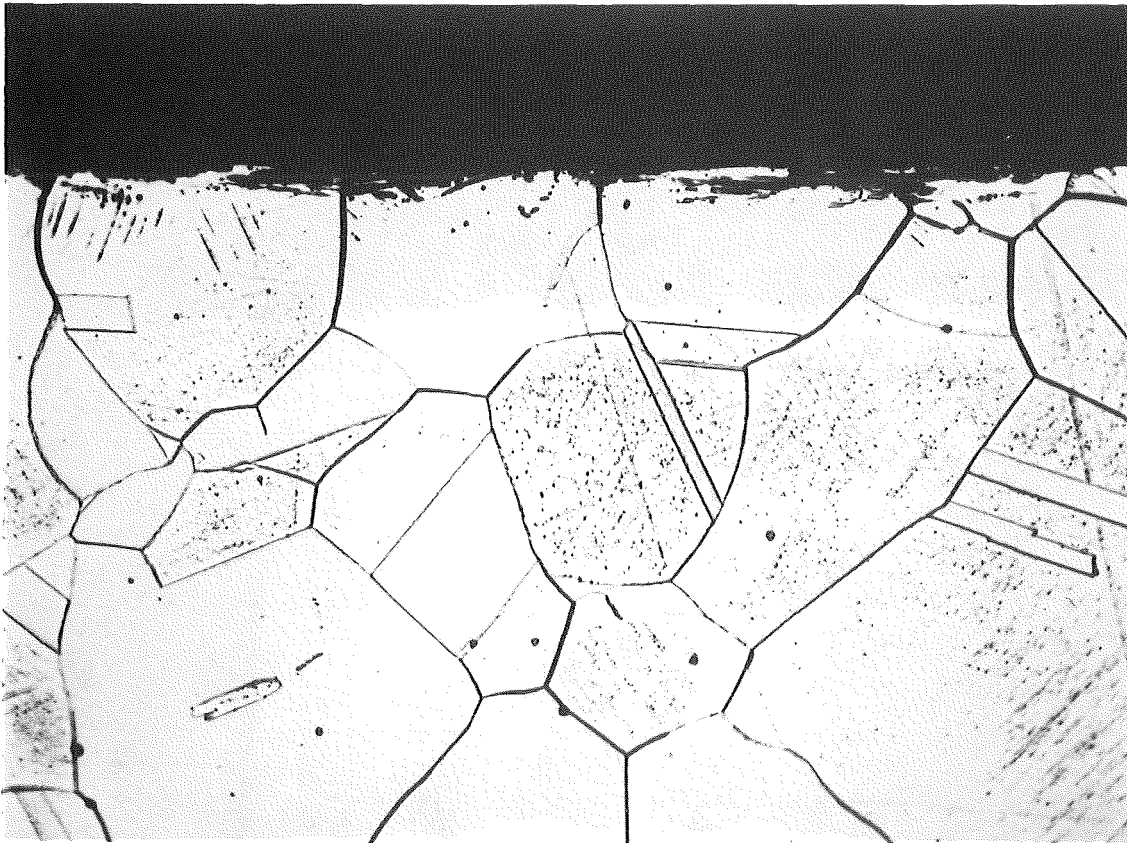


Fig. 11c: Reaction zone in the 316 L sample KfK 05-10, etched, magnif. 500 x

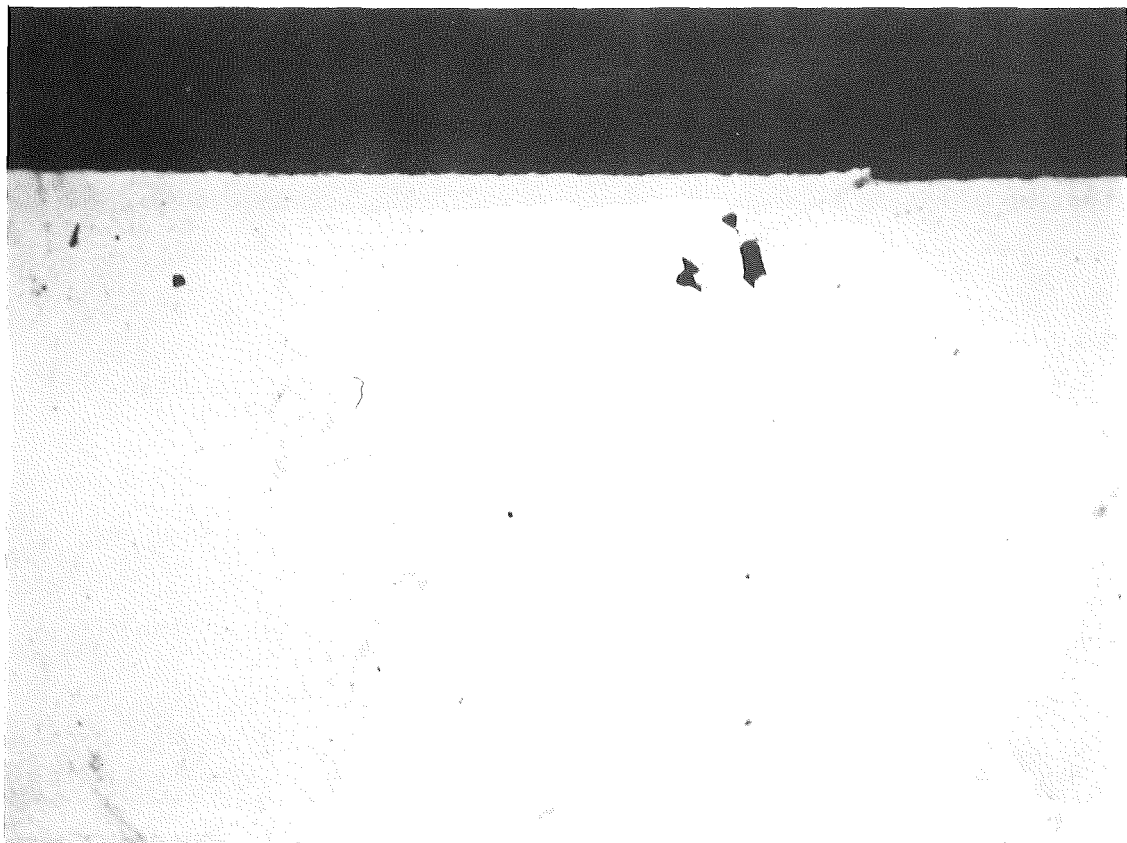


Fig. 12a: Surface in a cross-section of unirradiated beryllium, magnif. 500 x

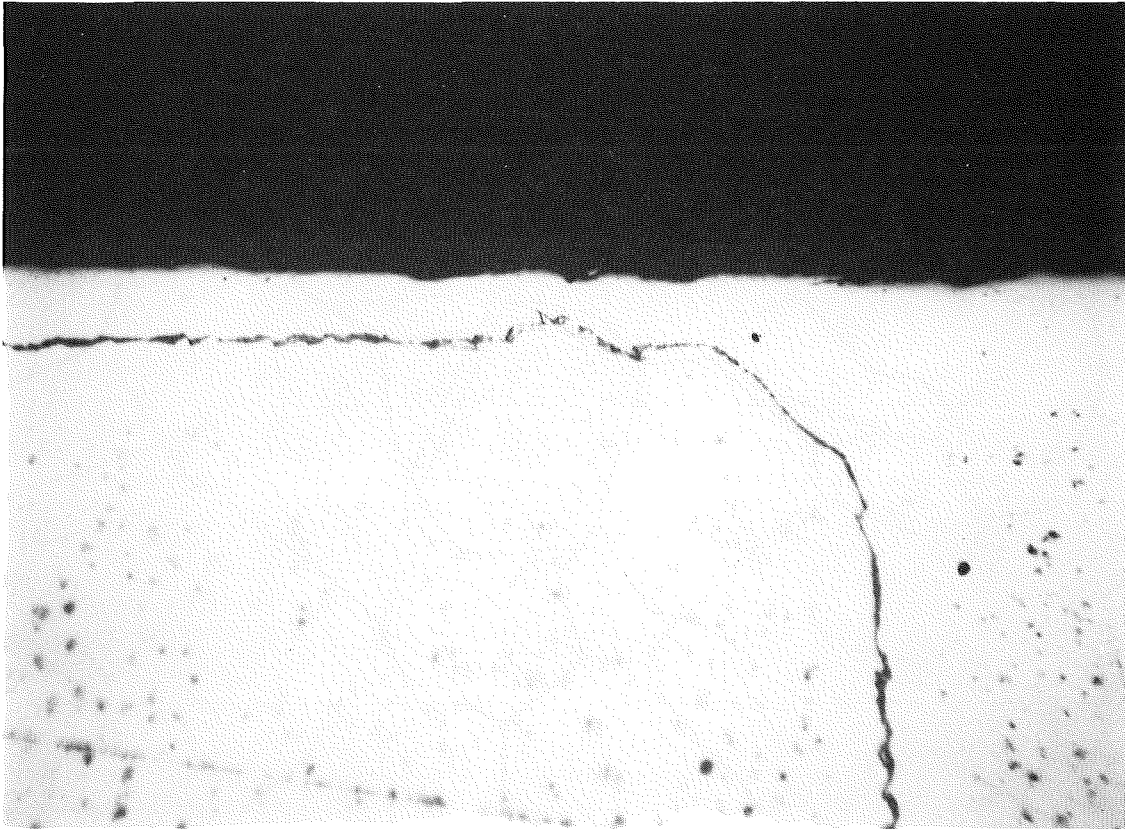


Fig. 12b: Surface roughening of the beryllium sample KfK 02-11 due to reaction with steel 316 L, magnif. 500 x

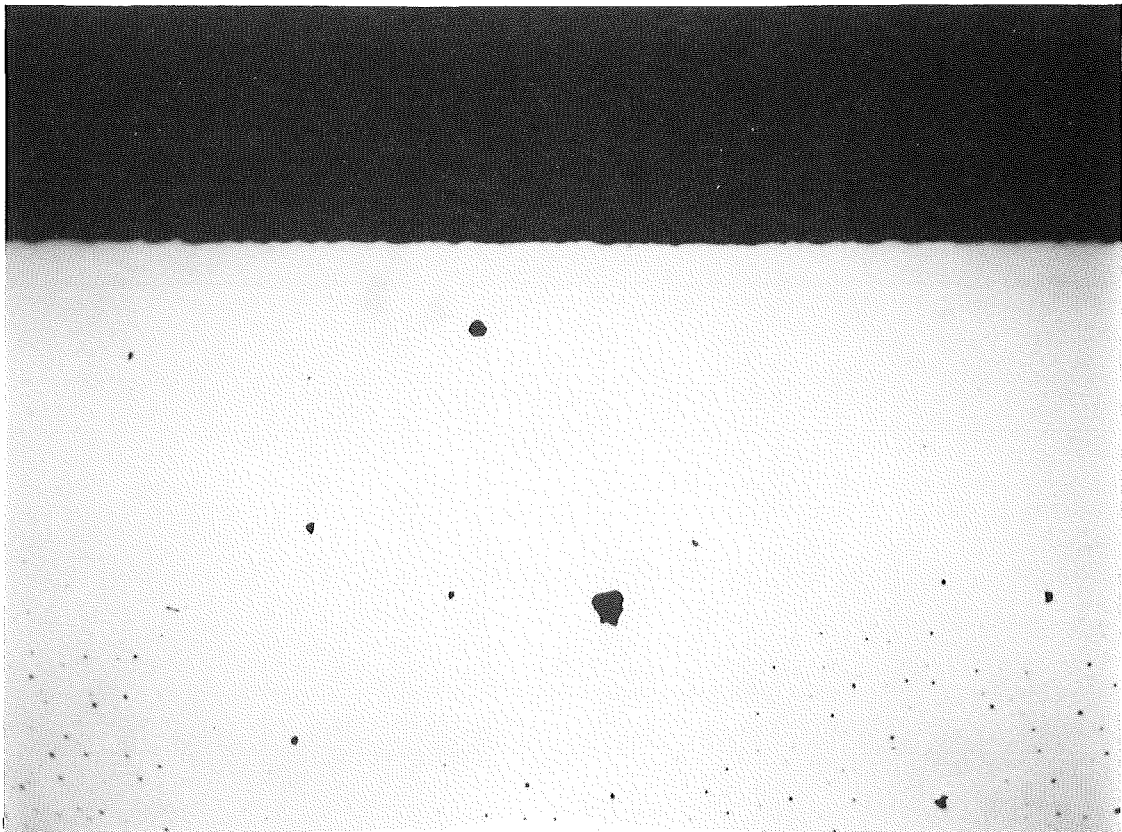


Fig. 12c: Minor surface roughening of the beryllium sample KfK 02-13 in contact with steel 1.4914, mangif. 500 x

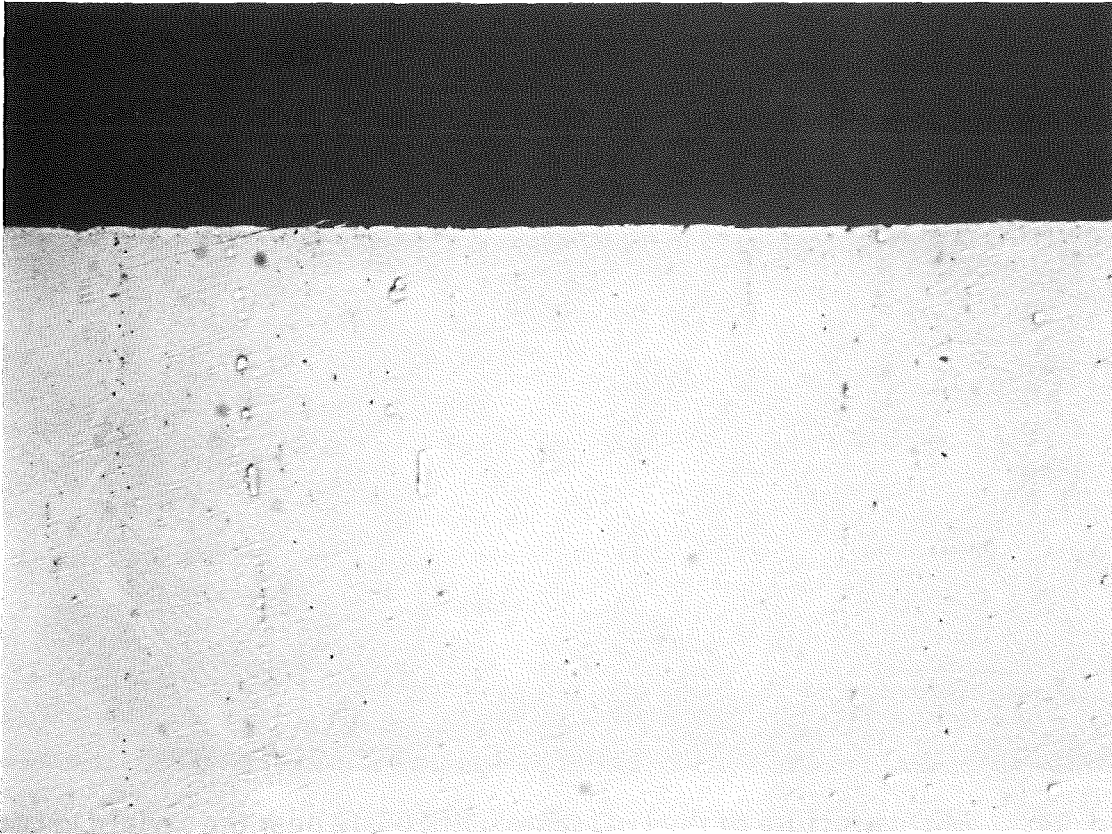


Fig. 13a: Surface in a cross-section of unirradiated steel 1.4914, magnif. 500 x



Fig. 13b: Surface roughening of the 1.4914 sample KfK 02-14 in contact with beryllium, magnif. 500 x

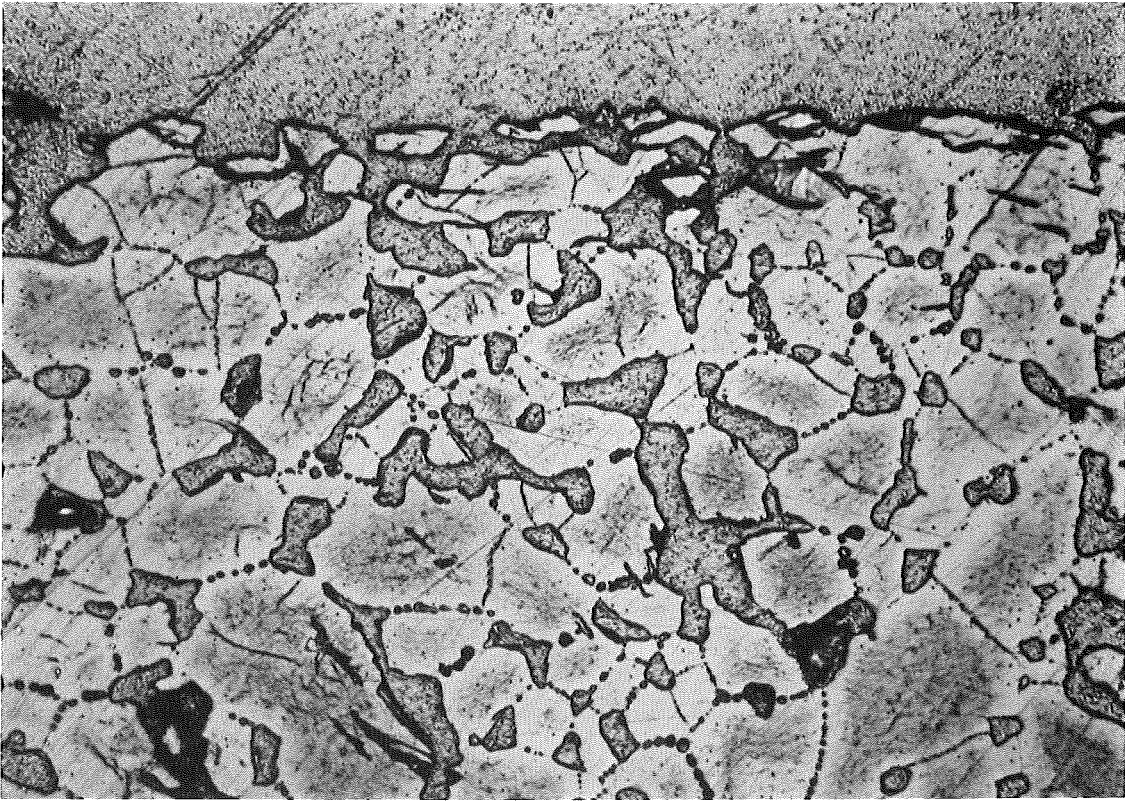


Fig. 14: Microstructure of the  $\text{Li}_2\text{O}$  sample KfK 05-12 near the surface in contact with beryllium, magnif. 500 x

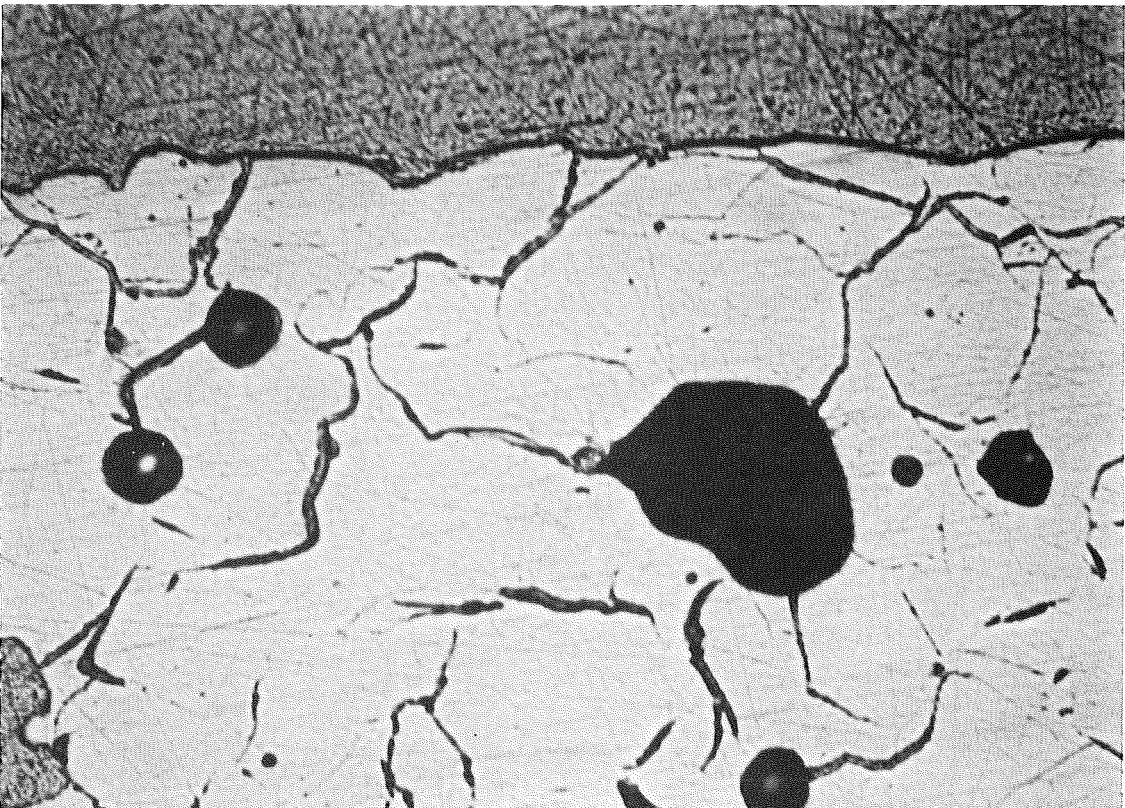


Fig. 15: Microstructure of the  $\text{Li}_4\text{SiO}_4$  sample KfK 02-12 near the surface in contact with beryllium, magnif. 500 x

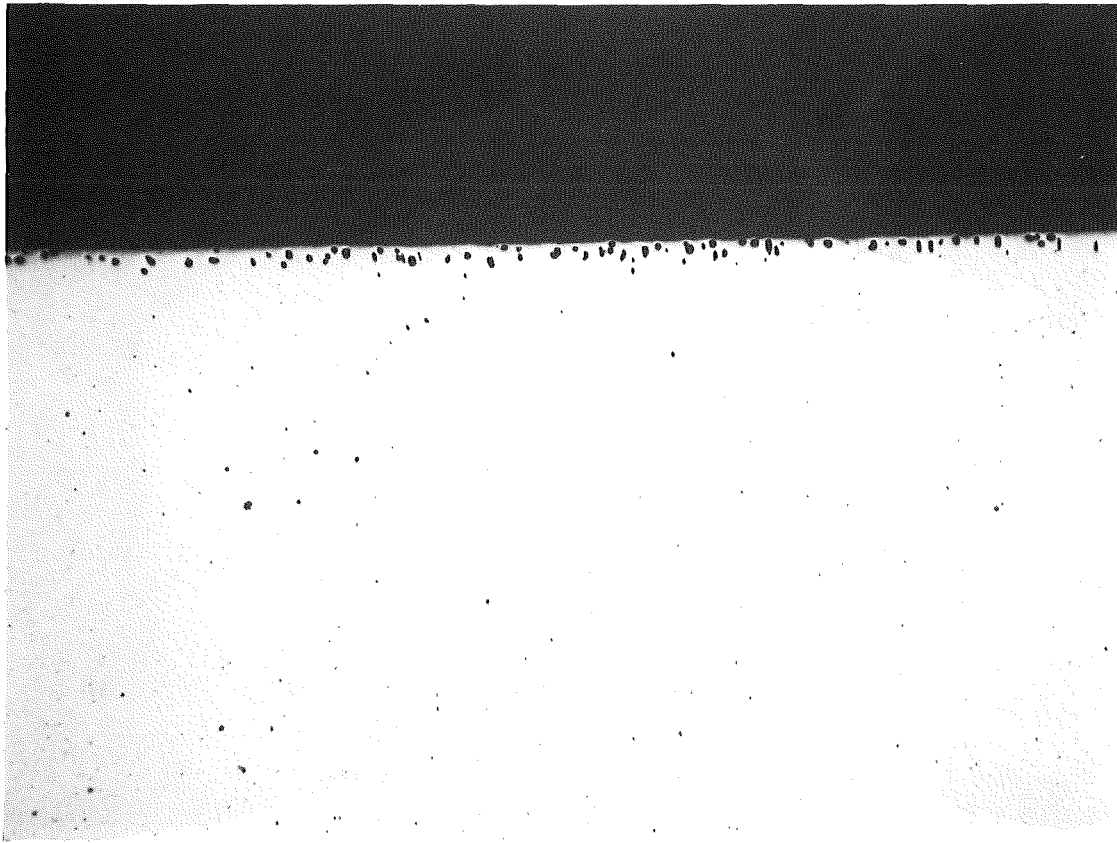


Fig. 16a: Porous zone near the surface of the beryllium sample KfK 05-11 in contact with  $\text{Li}_2\text{O}$  under neutron irradiation, magnif. 100 x

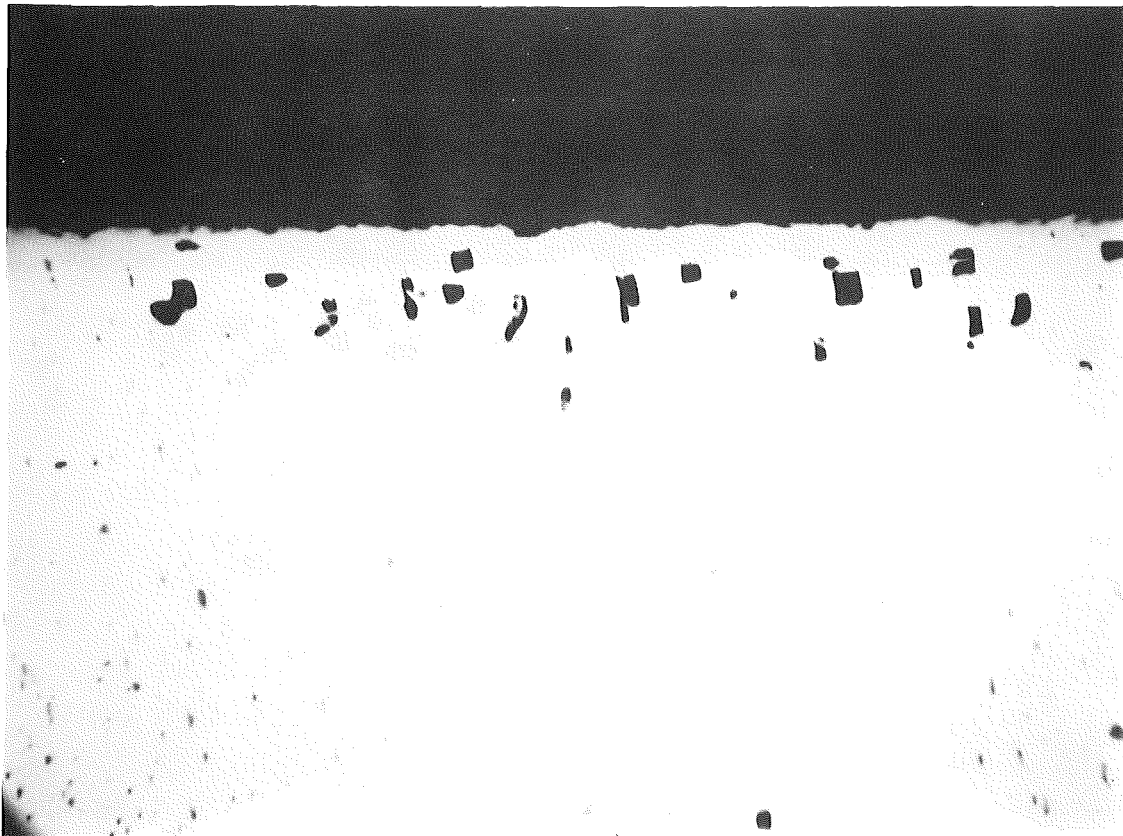


Fig. 16b: like 16a, magnif. 500 x

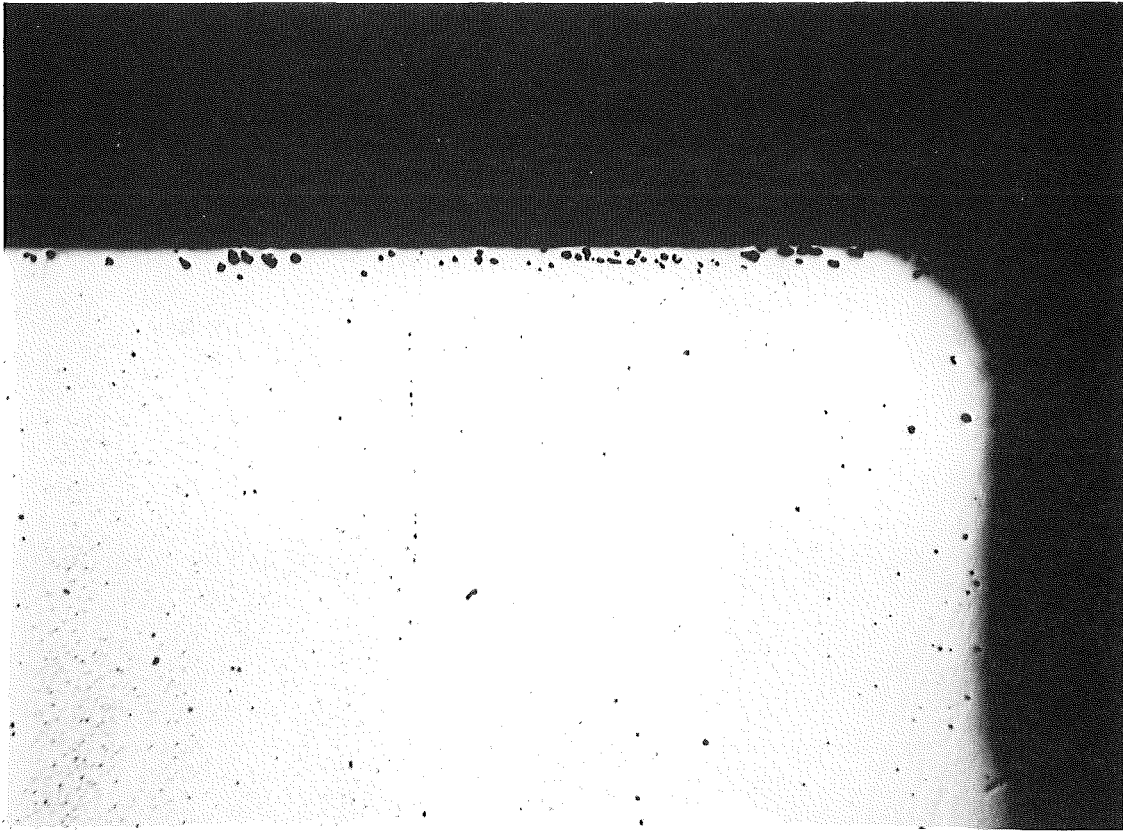


Fig. 17a: Porous zone near the surface of the beryllium sample KfK 05-13 in contact with  $\text{Li}_2\text{O}$  under neutron irradiation, magnif. 100 x

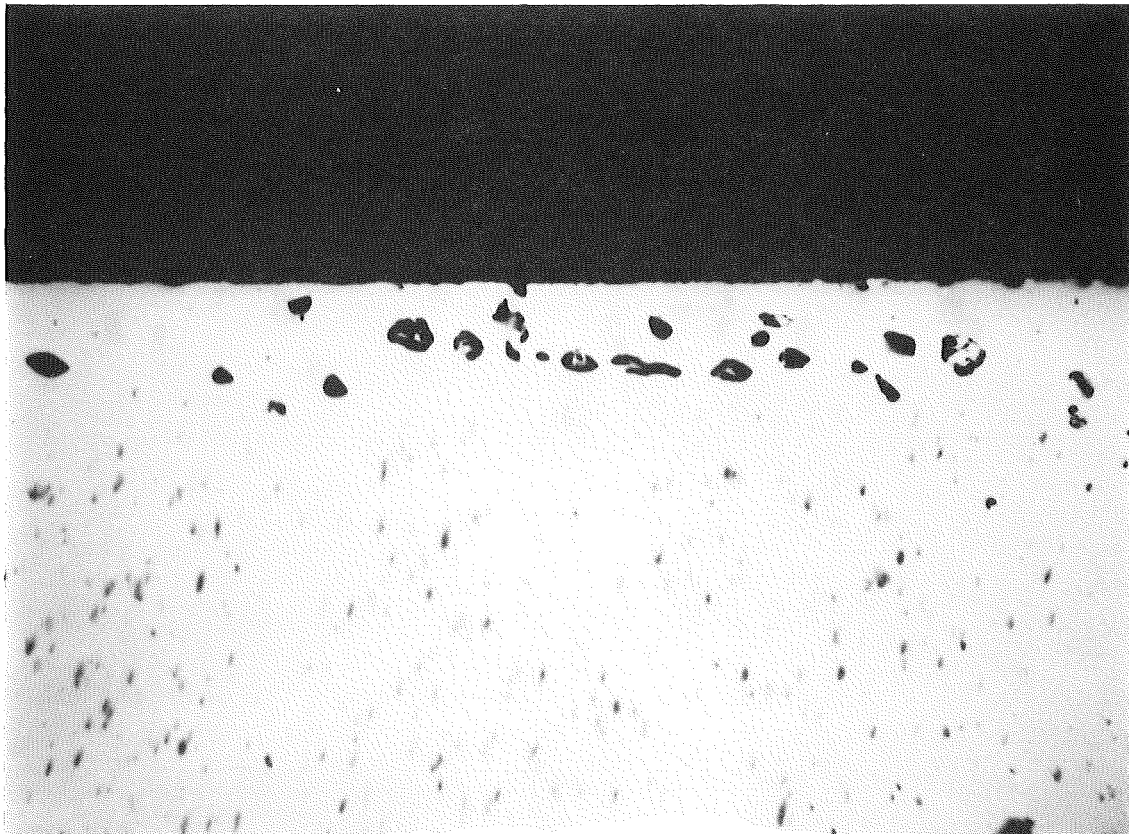


Fig. 17b: like 17a, magnif. 500 x

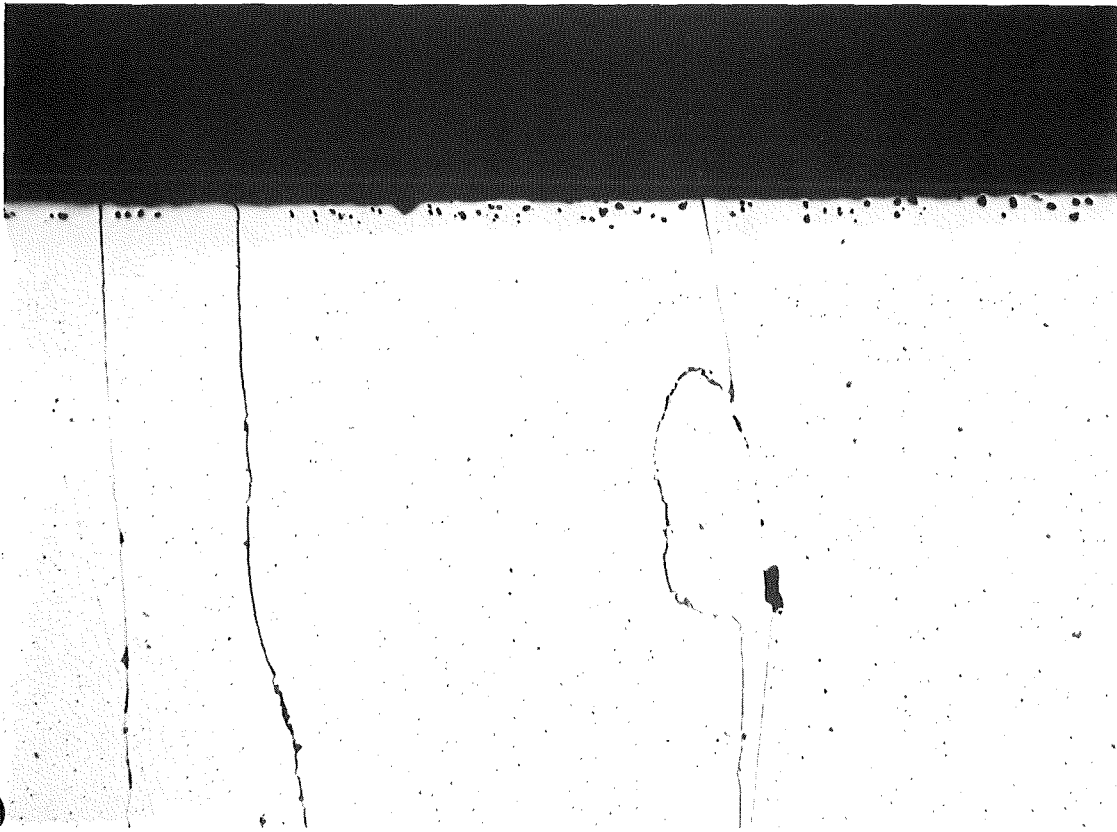


Fig. 18a: porous zone near the surface of the beryllium sample KfK 02-11 in contact with  $\text{Li}_4\text{SiO}_4$  under neutron irradiation, magnif. 100 x

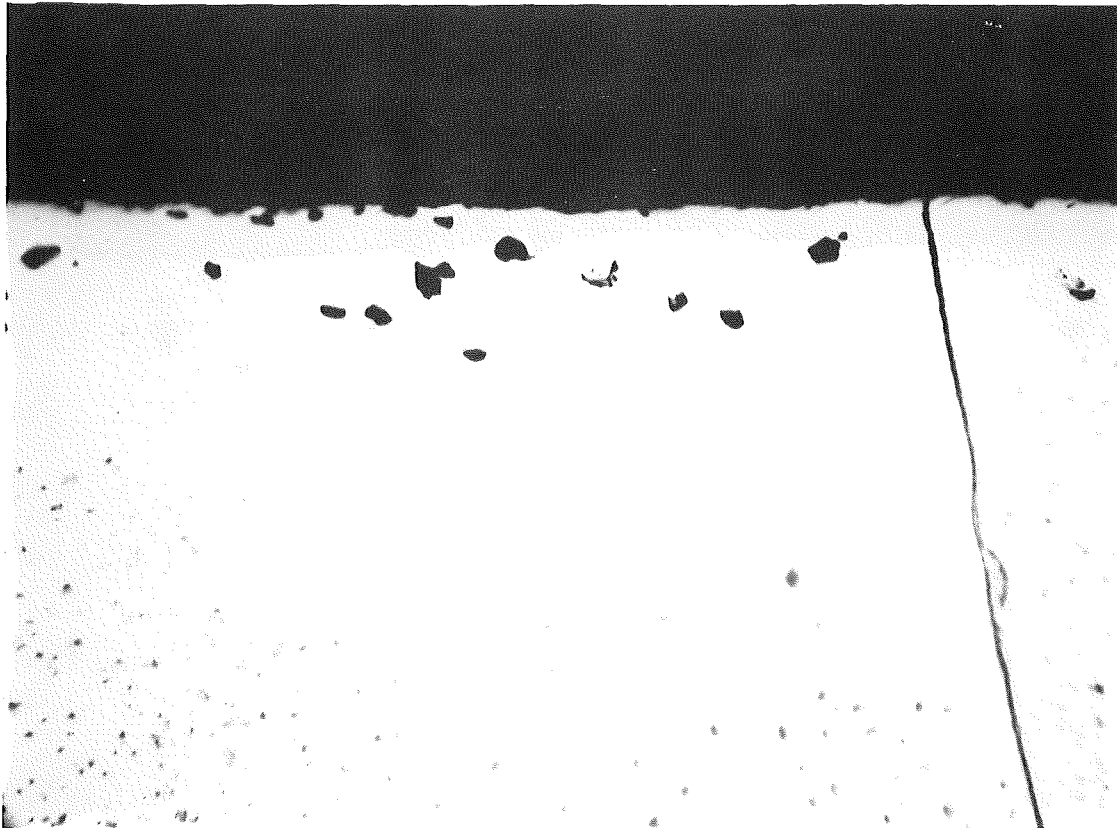


Fig. 18b: like 18a, magnif. 500 x

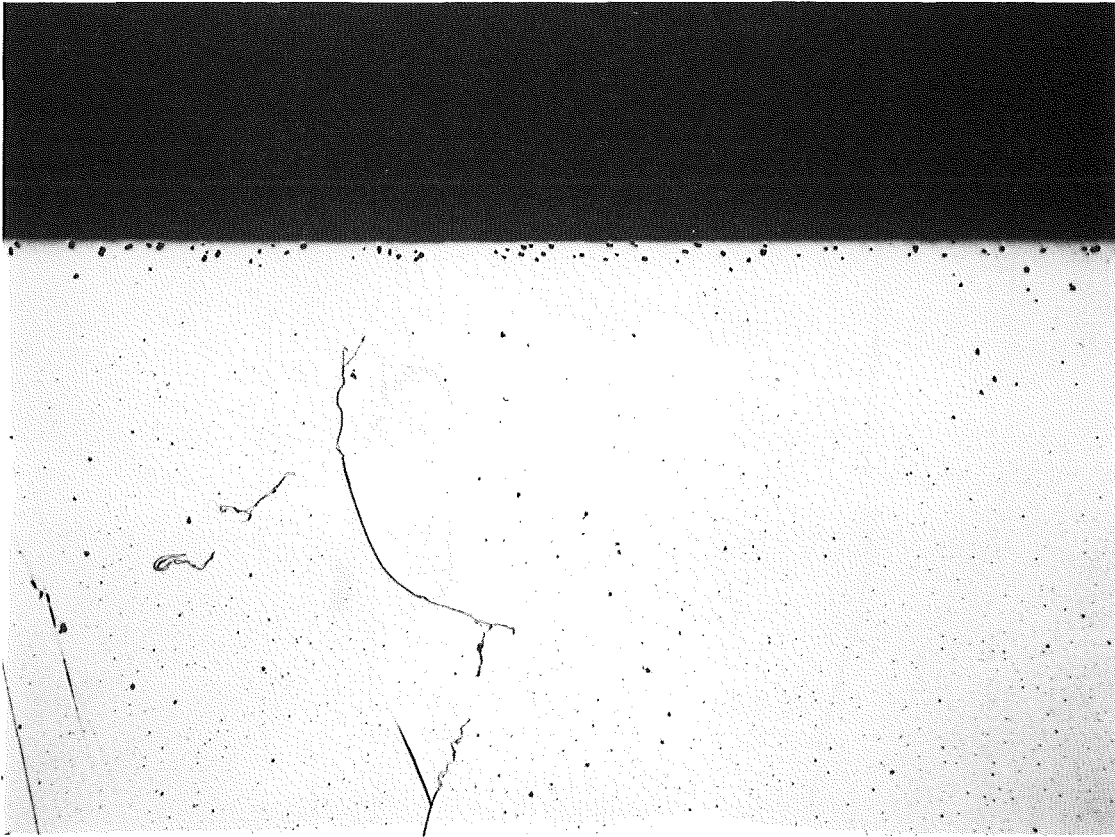


Fig. 19a: Porous zone near the surface of the beryllium sample KfK 02-13 in contact with  $\text{Li}_4\text{SiO}_4$  under neutron irradiation, magnif. 100 x



Fig. 19b: like 19a, magnif. 500 x